



**Improved Nuclear Site characterization for waste minimization
in DD operations under constrained Environment**

Research and Innovation action
NFRP-2016-2017-1

Statistical approach guide - UC1 Annex - Deliverable D3.7

Version n° 3

Authors: G. von Oertzen (Brenk), N. Pérot (CEA)

<http://insider-h2020.eu/>



*This project has received funding from the Euratom research and training programme 2014-2018 under the grant agreement n°755554 .
The content in this deliverable reflects only the author(s)'s views. The European Commission is not responsible for any use that may be made of the information it contains.*

Document Information

Grant Agreement #: 755554

Project Title: Improved Nuclear Site characterization for waste minimization in DD operations under constrained Environment

Project Acronym: INSIDER

Project Start Date: 01 June 2017

Related work package: WP 3: Sampling strategy

Related task(s):

Lead Organisation: Geovariances

Submission date:

Dissemination Level: Confidential

History

Date	Submitted by	Reviewed by	Version (Notes)
18 February 2021	G. von Oertzen		3
30 September 2021	G. von Oertzen		3



Table of contents

List of Tables	5
List of Figures	5
Annex 1: Liquid Waste Storage facility JRC Ispra (Use case 1)	7
1 Case introduction & overall strategy implementation	7
1.1 Case introduction: request for initial characterization	7
1.2 Objectives, highest priority	8
1.2.1 Define objectives	9
1.2.2 Highest priority objective	10
1.2.3 Further objectives.....	10
1.3 Constraints.....	11
1.4 Gather pre-existing records/data	11
1.5 Is data sufficient for analysis?	13
1.6 Various stages implementing the overall strategy: have more samples been collected?	13
2 Stage 1: Data analysis and sampling design.....	14
2.1 Pre-processing.....	14
2.2 Exploratory data analysis.....	14
2.2.1 Tank VA001.....	14
2.2.2 Tank VA002.....	20
2.2.3 Conclusion on the exploratory data analysis.....	25
2.3 Data analysis.....	26
2.3.1 Tank VA001.....	26
2.3.2 Tank VA002.....	32
2.4 Post processing: is objective achieved?	36
2.5 Sampling design	38
2.6 Conclusions on data analysis.....	39
3 Stage 2: Additional INSIDER measurements: data gathering, data analysis and comparison with stage 1 results	39
3.1 On-site comparison exercises.....	40
3.1.1 Dose rate measurements	40
3.1.2 Gamma spectrometry measurements	43
3.2 Sampling and in-lab intercomparison exercise.....	45
3.2.1 Benchmarking exercise on real samples	45
4 Stage 3: Comparison additional INSIDER measurements with data analysis on pre-existing data	46
4.1 Comparison between activity ratios based on in-situ with existing data.....	46
4.2 Uncertainty evaluation & sensitivity study	47
5 Lessons learnt and impact on the approach	47
6 Acronyms and abbreviations	50
7 Bibliography.....	50

List of Tables

Table 1: Liquid characteristics.....	9
Table 2: Artificial objectives based on WAC for selected waste form, waste product group and waste storage container	10
Table 3: List of radionuclides tested for in the preliminary sampling campaign, with number of measurements exceeding limit of detection (LOD), limits on maximum total specific activity and maximum total activity, as per WAC chosen. Radionuclides with all measurements below detection limit for both tanks shaded grey.	12
Table 4: Mean estimations with the different methods for the completely measured radionuclides and for radionuclides with limit of detection measurements in tank VA001.....	29
Table 5: 90%-quantile estimations with the different methods for the completely measured radionuclides and for radionuclides with limit of detection measurements in tank VA001.	30
Table 6: Estimation of probabilities to exceed two given thresholds with probabilistic risk bound method and with fitted theoretical distribution laws for radionuclide activities of tank VA001..	32
Table 7: Mean estimations with the different methods for the measured radionuclides in VA002 tank.	34
Table 8: 90%-quantile estimations with the different methods for the measured radionuclides in tank VA002.....	35
Table 9: Estimation of probabilities to exceed 2 given thresholds with probabilistic risk bound method and with fitted theoretical distribution laws for radionuclide activities of tank VA002.....	36
Table 10: Estimate of maximum total activity per nuclide, tank VA001, based on maxima measured for specific activity per nuclide and estimated total solids.....	37
Table 11: Estimate of maximum activity per nuclide, tank VA002.....	37
Table 12: Summary of dose rate measurements performed in the in situ campaign.....	41
Table 13: Summary of gamma spectrometry measurements (November 2019)	44
Table 14: Measurement uncertainty from comparison on CRM1	46

List of Figures

Figure 1: Schematic of tank farm building	8
Figure 2: Radionuclide analysis (tank VA001): beta and alpha activity concentration (primary axis: ²⁴¹ Pu, secondary axis: all other nuclides)	15
Figure 3: Radionuclide analysis (tank VA001): gamma activity concentration	15
Figure 4: Histograms for the eight completely measured radionuclides in tank VA001 (status 2012).	16
Figure 5: Boxplots for the eight completely measured radionuclides in tank VA001 (status 2012).	17
Figure 6: Linear correlations between the eight completely detected radionuclides in tank VA001, linear scale (status: 2012).	18
Figure 7: Linear correlations with outliers removed, tank VA001, status 2012.	19
Figure 8: Variable projection on the first two principal components for radionuclide activities of VA001.....	20
Figure 9: Radionuclide analysis (tank VA002, status 2013): beta and alpha activity concentration (primary axis: ⁹⁰ Sr, ²⁴¹ Pu and ²⁴¹ Am, secondary axis: all remaining nuclides).....	21
Figure 10: Radionuclide analysis (tank VA002, status 2013): gamma activity concentration (secondary axis: ¹³⁷ Cs)	21
Figure 11: Histograms for the measured radionuclides in tank VA002 (2013).	22

Figure 12: Boxplot for the measured radionuclides in tank VA002 (2013).	23
Figure 13: Linear correlations between the measured radionuclides in tank VA002.	24
Figure 14: Variable projection on the first two principal components for radionuclide activities of tank VA002.....	25
Figure 15: Mean bootstrap estimation as a function of the number of replicates for the eight measured radionuclides in tank VA001 (status 2012).	27
Figure 16: Mean bootstrap estimation as a function of the number of replicates for ^{241}Pu , ^{238}Pu , $^{239+240}\text{Pu}$ and ^{241}Am in tank VA001 with (left) and without outliers (right).	28
Figure 17: Difference between estimations with and without uncertainties and limit of detection specific treatment for radionuclide activities in tank VA001.	30
Figure 18: Mean estimations with the different methods for radionuclide activities in VA001 tank.	31
Figure 19: 90%-quantile estimations with the different methods for radionuclide activities in VA001 tank.....	31
Figure 20: Mean bootstrap estimation varying with the size of the replicates for the measured radionuclides in tank VA002.....	33
Figure 21: Difference between estimates with and without uncertainties for radionuclide activities in tank VA002.	35
Figure 22: Measurement positions on the tanks for dose rate measurements.....	41
Figure 23: Dose rate measurements, UC1 (left: tank VA001, right: tank VA002).....	42
Figure 24: Vertical (left) and horizontal (right) dose rate profiles in both tanks	43
Figure 25: Measurement positions for gamma spectrometry measurements (left: tank VA001, right: tank VA002).....	43
Figure 26: Activity ratio $^{137}\text{Cs}/^{60}\text{Co}$ in the two tanks, as determined by gamma spectrometry	45
Figure 27: Comparison of activity ratio $^{137}\text{Cs}/^{60}\text{Co}$ between gamma spectrometry measurements and existing data (extrapolated to November 2019)	47

Annex 1: Liquid Waste Storage facility JRC Ispra (Use case 1)

In this annex, use case 1 (UC1), consisting of a small data set from two tanks containing low-level liquid waste at the JRC Ispra site in Italy is discussed. In chapter 1, we introduce the use case and place it within the context of the overall strategy implementation. In chapter 2, the pre-existing data is analysed with the aim of formulating the sampling design. Additional activities within the INSIDER project such as on-site comparison exercises and in-lab intercomparison exercises are summarised in chapter 4 and discussed in chapter 5. We conclude the annex with a summary of lessons learnt in chapter 5.

1 Case introduction & overall strategy implementation

In this chapter, we introduce the use case. In the absence of existing objectives, we formulate artificial objectives for the characterization campaign, summarise the constraints and analyse the existing data in view of the overall strategy implementation.

1.1 Case introduction: request for initial characterization

UC1 refers to the characterization of two tanks containing liquid low level waste (LLLW) at the liquid waste storage facility at the JRC site of Ispra, Italy (Figure 1). The contents of the tanks originates from the old liquid effluent treatment station associated with the nuclear research facility, which included a nuclear reactor, and is destined to be routed for cementation or alternative solidification and conditioning treatment with the aim of disposal.

The liquid waste is contained in two tanks, each about 50 m³ in volume, containing sludge with a high water content. The specific activities of radionuclides contained are between a few tenths to just over 100 Bq/g (at the time of the initial analysis, which was performed in the years 2012 and 2013 respectively) for relevant nuclides, which include gamma emitters ⁶⁰Co, ¹³⁷Cs and ²⁴¹Am as well as alpha-and beta emitters. The tanks are denoted VA001 and VA002.

In terms of the overall strategy implementation, the request for initial characterization is the decision by the operator to change the status of the waste. For this, the waste has to be characterized according to the intended end points (objectives) of the waste.

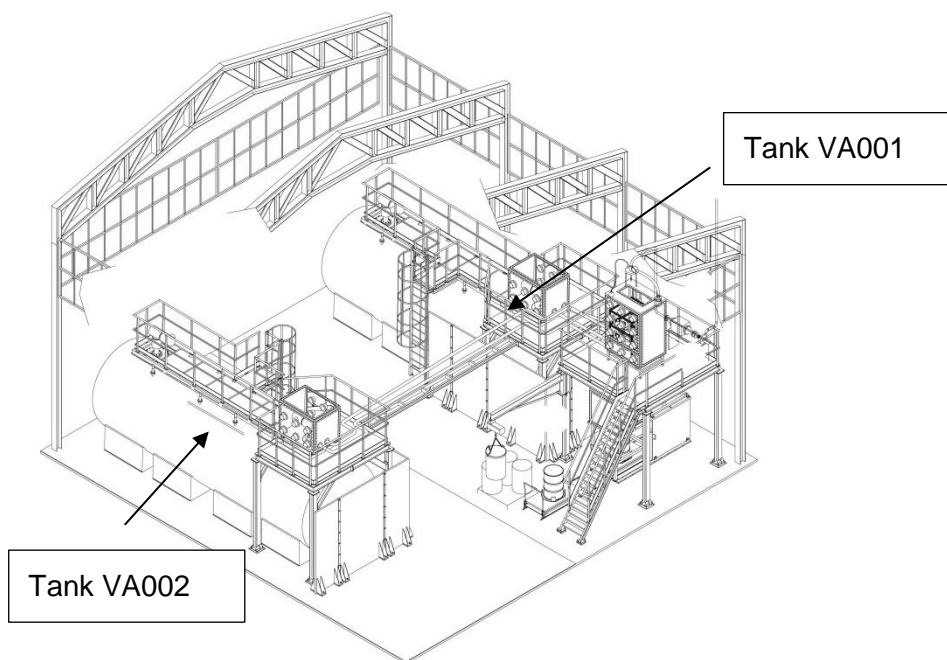


Figure 1: Schematic of tank farm building

1.2 Objectives, highest priority

The licensee has not specified any waste acceptance criteria for this waste. Moreover, no information is available on what the conditioning process prior to waste acceptance should be. In order to collect relevant information on the historical background of the site and on the objectives for the characterization campaign, a questionnaire was issued to the operators. At the time of the initial filling of the tanks, sludge samples from both tanks were collected and analysed for radionuclide content.

In order to be able to compare the outcomes of the characterization campaign with the objectives, we defined artificial objectives and waste acceptance criteria based on an assumed conditioning process. Possible objectives include:

1. Decision about clearance of the selected and measured material.
2. Characterization of the material for the further decision process with respect to total activity, nuclide composition or nuclide vector (NV), especially ratio of difficult-to-measure nuclides (DTM nuclides) or dose rate;
3. Decision if material will meet the waste acceptance criteria (WAC) for transport, conditioning process, interim storage or final disposal; or
4. Balancing of activities within transfer of ownership between different license owners on national or international requirements.

For each of the possible objectives, different approaches may be necessary. For example, for objective No. 1, the final activity concentration is to be determined with the confidence level prescribed by regulatory framework (typically 95 %) not to exceed the clearance level for a defined average size (mass or surface). For objective No. 4, in contrast, only the best estimate of the total activity is required. The characterization of material (objective No. 2) is often an intermediate

objective required for deciding on the final objective. Depending on that objective, the statistical approaches may be different. With respect to the determination of NV for DTM nuclides, the accuracy of determination of DTM nuclides and the different radiological impact of the nuclides with respect to the final objective have to be considered.

1.2.1 Define objectives

Waste acceptance criteria are in many cases the final objective of any statistical calculation. We have therefore selected objective No. 3 from the list above and will not further consider the other possible objectives in the next stages. In order to make the example as realistic as possible, the WAC as specified for disposal in *Endlager Konrad* (deep geological disposal site for low and intermediate level waste in Germany, licensed and under construction) are applied here ([Brennecke, 2015](#)). The WAC are then grouped into those referring to the package (dose rate, surface contamination and pressure-free delivery) and those referring to the package contents, assuming the waste product group and the waste container have been decided upon. The package contents are to be solid, not subject to fouling, free from liquids and gases, free from explosive or flammable materials, may not contain fissile materials with the exception of uranium up to 50 g per 0.1 m³ of product. In addition, for each product group the specified activity limits are not to be exceeded. The assumption made here is that the liquids will be evaporated by heating. The objective then is to adequately characterize the waste by determining the chemical and physical properties of the waste as well as the radiological properties to check if the WAC can be met.

Inspection of the existing data relating to its chemical characteristics, as summarised in Table 1, reveals that the water content of the sludge in the containers is high, which means that the volume could be reduced by evaporation to fit the standardised cast iron type III container, which has a net volume of 1 m³, with an allocation to waste product group APG (“Abfallproduktgruppe”) 06 (concentrates). We’ll assume here that the evaporated contents of each tank will fit into the container type specified. This is a conservative assumption, as meeting the WAC for one container automatically ensures the WAC are met should two containers per tank be required instead. The same applies if the conditioning process involves cementation of the solidified waste, which would result in higher volumes and therefore lower activities per waste container utilized.

Table 1: Liquid characteristics

	VA001	VA002
Volume (m ³)	44,6	37,5
pH	7,8	7,7
water content (%)	99	94,8
total solids (mg/g)	5,5	52,6
total solid (kg)	245,3	1972,5
U (ppm)	19,6	not given
total organic carbon (ppm)	811,7	272,5
bulk density (g/mL)	1	1,1

The WAC relating to the radiological characterization are then the activity limits relating to the identified product group and waste container. These are summarised in Table 2 based on the

selected product group and waste container according to the WAC for the Konrad repository, and listing only the nuclides detected in the existing data where relevant.

Table 2: Artificial objectives based on WAC for selected waste form, waste product group and waste storage container

	WAC	
package	average dose rate, contact	< 0.002 Sv/h
	average dose rate, at 1 m	< 0.0001 Sv/h
	surface contamination, alpha nuclides with clearance limit 5000 Bq	< 0.5 Bq/cm ²
	surface contamination, beta nuclides with clearance limit 5 MBq	< 50 Bq/cm ²
	surface contamination, other nuclides	< 5 Bq/cm ²
	internal pressure	< 1.2 bar
product		solid
		not rotting or fermenting
		no liquids or gases
		no flammable or explosive substances
	²³³ U, ²³⁵ U, ²³⁹ Pu, ²⁴¹ Pu, ^{242m} Am, ²⁴³ Cm, ²⁴⁷ Cm, ²⁴⁹ Cf, ²⁵¹ Cf	< 50 g/0.1m ³
product group: APG 06 (concentrates)	¹⁴ C	< 2.1 E15 Bq
	⁴¹ Ca	< 1.6 E13 Bq
	⁵⁹ Ni	< 7.6 E14 Bq
	⁶⁰ Co	< 5.0 E12 Bq
	⁶³ Ni	< 7.0 E14 Bq
	⁵⁵ Fe	< 1.4 E16 Bq
	⁹⁰ Sr	< 8.6 E11 Bq
	⁹⁹ Tc	< 5.4 E13 Bq
	¹²⁹ I	< 4.3 E08 Bq
	¹³⁷ Cs	< 5.1 E12 Bq
	²³⁸ U	< 2.4 E12 Bq
	²³⁸ Pu	< 8.9 E11 Bq
	²⁴¹ Pu	< 1.7 E13 Bq
	²³⁹⁺²⁴⁰ Pu	< 8.3 E11 Bq
	²⁴¹ Am	< 7.6 E11 Bq
	²⁴⁴ Cm	< 1.4 E12 Bq

1.2.2 Highest priority objective

The **highest priority objective** here is to characterize the radionuclide content of the tanks, in view of deciding if the WAC for the selected waste category can be met (i.e. if the maximum activity of any nuclide exceeds the value set in the WAC).

1.2.3 Further objectives

In view of the intended end point of the waste, i.e. conditioning with the aim of disposal, the remaining objectives refer to the WAC defined. With radiological parameters identified as the highest priority, the remaining objectives refer to meeting the criteria for the waste group decided upon: The waste

package contents are to be solid, not subject to fouling, free from liquids and gases, free from explosive or flammable materials, may not contain fissile materials with the exception of uranium up to 50 g per 0.1 m³ of product. These objectives are to be met for the conditioned package.

1.3 Constraints

For the characterization of the sludge in the two tanks, the constraints include

1. Sampling access: Access to the tanks for in-situ measurements is limited due to the presence of a shielding wall against one of the tanks and the location of the tanks close to the wall of the building. Destructive sampling is restricted to sampling in-stream while pumping the contents through a loop, i.e. it is not possible to access any desired volume within the tank for sampling.
2. Homogenisation of tanks contents, settling: Although a stirring mechanism is available for homogenising the tanks contents, solids have deposited at the bottom of one or both tanks, which may not be mobilisable by stirring.
3. The non-availability of suitable reference samples with adequate solid fraction for characterizing the sludge is a contributing factor to the uncertainty.
4. No clear characterization objectives have been defined. The assumed waste acceptance criteria will therefore introduce additional uncertainty as several assumptions have been made about the conditioning process and the waste form. For the purpose of the strategy, the objectives are assumed to be those for conditioning for disposal and amount to the estimation of the total activity acceptable for each nuclide present.

1.4 Gather pre-existing records/data

A total of 12 sludge samples from each tank were collected shortly after the tanks were filled, in November 2012 (tank VA001) and February 2013 (tank VA002), and chemical and radionuclide analysis was performed. The basis of the sampling at the time was that the tank content was supposed to be homogeneous (i.e. no settling of solids had yet occurred, and the contents were stirred prior to sampling). The representativity of the samples is investigated and discussed in view of the sampling design strategy in chapter 2.

Subsequent to the initial sampling campaign, it is suspected that settling of the contents has occurred which may have solidified at the bottom, resulting in inhomogeneous distribution of contents of the sludge.

The set of 12 samples each was drawn immediately following the filling of the two tanks, and after stirring the contents. Consequently, water content of the samples is high as there has been no separation of solids within the tank contents. In the meantime, settling deposition may have occurred at the bottom of the tanks. The samples collected, 600-700 ml in volume each, were analysed for chemical characteristics, elemental composition, granulometry of solids and radiological content. Radiological analysis included liquid scintillation counting (LSC), gamma spectroscopy (GS), low

energy gamma spectroscopy (LEGS) and alpha spectroscopy (AS) for select radionuclides. Radionuclides tested and those detected in the samples are summarised in Table 3. Based on the total volume of sludge in the tanks and the bulk density, the specific activity limit to be satisfied in the WAC can be estimated. This is summarised in Table 3, where we indicate the number of measurements exceeding the limit of detection, the limit on maximum activity for the tanks as per WAC and the limit of specific activity resulting from the WAC if extrapolated using the known volume and bulk density of the sludge. These values can then be compared to the sample specific activities, which are also expressed in Bq/g of sludge rather than in Bq/ml.

Table 3: List of radionuclides tested for in the preliminary sampling campaign, with number of measurements exceeding limit of detection (LOD), limits on maximum total specific activity and maximum total activity, as per WAC chosen. Radionuclides with all measurements below detection limit for both tanks shaded grey.

Radio-nuclide	No. of measurements > LOD		Specific activity limits based on WAC and volume of sludge in tanks, Bq/g of sludge		WAC (maximum total activity limit, Bq)
	Tank VA001	Tank VA002	Tank VA001	Tank VA002	
¹⁴ C	0	12	4.7E+07	5.1E+07	2.1E+15
⁴¹ Ca	0	0	3.6E+05	3.9E+05	1.6E+13
⁵⁵ Fe	5	0	3.1E+08	3.4E+08	1.4E+16
⁵⁹ Ni	0	0	1.7E+07	1.8E+07	7.6E+14
⁶⁰ Co	12	12	1.1E+05	1.2E+05	5.0E+12
⁶³ Ni	5	12	1.6E+07	1.7E+07	7.0E+14
⁷⁹ Se	0	0	1.6E+04	1.7E+04	7.0E+11
⁹⁰ Sr	12	12	1.9E+04	2.1E+04	8.6E+11
⁹³ Mo	0	0	1.7E+06	1.8E+06	7.6E+13
⁹³ Zr	0	0	5.4E+06	5.8E+06	2.4E+14
⁹⁴ Nb	0	0	4.9E+03	5.3E+03	2.2E+11
⁹⁹ Tc	0	12	1.2E+06	1.3E+06	5.4E+13
¹⁰⁷ Pd	0	0	2.5E+07	2.7E+07	1.1E+15
¹²⁹ I	0	0	9.6E+00	1.0E+01	4.3E+08
¹³⁴ Cs	0	0	4.3E+05	4.6E+05	1.9E+13
¹³⁷ Cs	12	12	1.1E+05	1.2E+05	5.1E+12
¹⁴⁷ Pm	0	0	1.4E+08	1.6E+08	6.4E+15
¹⁵¹ Sm	0	0	2.7E+08	2.9E+08	1.2E+16
¹⁵² Eu	0	0	9.9E+04	1.1E+05	4.4E+12
¹⁵⁴ Eu	0	0	1.4E+05	1.5E+05	6.3E+12
²³⁵ U	0	0	5.4E+04	5.8E+04	2.4E+12
²³⁸ U	12	12	5.4E+04	5.8E+04	2.4E+12
²³⁷ Np	0	0	3.1E+02	3.4E+02	1.4E+10
²³⁸ Pu	12	12	2.0E+04	2.2E+04	8.9E+11
^{239/240} Pu	12	12	1.9E+04	2.0E+04	8.3E+11

Radio-nuclide	No. of measurements > LOD		Specific activity limits based on WAC and volume of sludge in tanks, Bq/g of sludge		WAC (maximum total activity limit, Bq)
	Tank VA001	Tank VA002	Tank VA001	Tank VA002	
²⁴¹ Pu	12	12	3.8E+05	4.1E+05	1.7E+13
²⁴¹ Am	12	12	1.7E+04	1.8E+04	7.6E+11
²⁴⁴ Cm	0	12	3.1E+04	3.4E+04	1.4E+12

The detection limit for alpha, beta or gamma emitting nuclides in these sample analyses ranged approximately between 0.01 and 0.5 Bq/g, for both data sets, see ([Londyn P., 2013a](#)) and ([Londyn, P. 2013b](#)).

1.5 Is data sufficient for analysis?

Apart from the radiological characteristics, which are discussed further in chapter 2 below, the pre-existing data relating to particle size distribution, chemical composition and chemical characteristics seem to give a representative indication of a fairly homogenous physico-chemical content of the tanks, where this information is available. This confirms the initial assessment of the highest priority objective, i.e. the determination of the radionuclide content of the tanks including spatial distribution thereof (if any).

The pre-existing data provides sufficient scope for data analysis.

1.6 Various stages implementing the overall strategy: have more samples been collected?

We could only use the pre-existing data to implement the data analysis and sampling design strategy developed within the INSIDER project. The pre-existing data consisted of results from chemical and radionuclide analysis for a total of 12 sludge samples from each tank, collected shortly after the tanks were filled in the years 2012 and 2013. The overall strategy implementation is carried out in two stages:

- Stage 1: Preliminary data analysis on the pre-existing data followed by a decision if objectives are met. This is followed by a sampling design if objectives are not met. For this use case, the sampling design was not necessary to gather additional data, but was developed nevertheless, for the purpose of the exercise.
- Stage 2: Execution of the sampling design and analysis of the data. It should be emphasised that due to the logistics of the INSIDER project, the proposed sampling design was not carried out. Instead, a pre-determined set of sampling exercises was performed, both in-situ and as an inter-laboratory comparison exercise. These are explained in more detail in the relevant work package deliverables, but are also summarised in section 3.
- Stage 3: Comparison of original and additional data and evaluation.



During the INSIDER project, an on-site inter-comparison measurement campaign was performed and new samples were taken and distributed to different European laboratories for comparing the lab results. Since we did not have any impact on the sampling design, those results are not reported here as a second loop of the strategy implementation. They are reported as additional INSIDER measurements and compared with the results of the data analysis of the pre-existing data.

2 Stage 1: Data analysis and sampling design

The pre-existing data for this exercise originated from the once-off initial sampling campaign shortly after filling the tanks.

The laboratory dates for the sample sets are February 2013 for tank VA002 and November 2012 for tank VA001. These dates refer to the analysis results of the 12 samples each per tank. In addition, the maximum contact dose rate on any of the two tanks is recorded as 30 $\mu\text{Sv/h}$. No further information about dose rates or homogeneity of the tank contents is available a priori. There is also no information about applicable scaling factors for the waste.

Based on the operational history, the liquid waste is effluent from a nuclear research facility which included the operation of a research reactor.

2.1 Pre-processing

The data set is small (only 12 data points or samples for each of the two tanks). A few outliers can be identified, but are kept as a decision on the representativeness cannot be made at this point. Nevertheless, we proceed with the exploratory data analysis.

2.2 Exploratory data analysis

As shown in Table 3, the nuclides found to be present with detectable activities in the tanks include alpha- and beta-emitting nuclides ^{238}U , ^{241}Pu , ^{99}Tc , ^{90}Sr , ^{63}Ni , ^{14}C , ^{238}Pu , $^{239+240}\text{Pu}$ and ^{241}Am as well as the gamma-emitting nuclides ^{60}Co and ^{137}Cs . Gamma-emitter ^{241}Am was only tested for and detected in tank VA002. Of these, the radionuclides with the highest activities were ^{90}Sr , ^{241}Pu , ^{137}Cs and ^{241}Am . The specific activities in the sludge samples from tank VA002 were slightly higher than in tank VA001. As the time elapsed since waste generation is more than 10 years, probably significantly so, very short living nuclides are no longer expected to be present. Activities were found to be below detection limit for many of the nuclides.

Further data analysis is described separately for each tank.

2.2.1 Tank VA001

For tank VA001, we start the analysis of the radionuclide content by visually inspecting the trends of the nuclides found to be above the detection limit on all 12 samples. The alpha and beta activities are summarised in Figure 2, the nuclides detected using GS are shown separately in Figure 3.

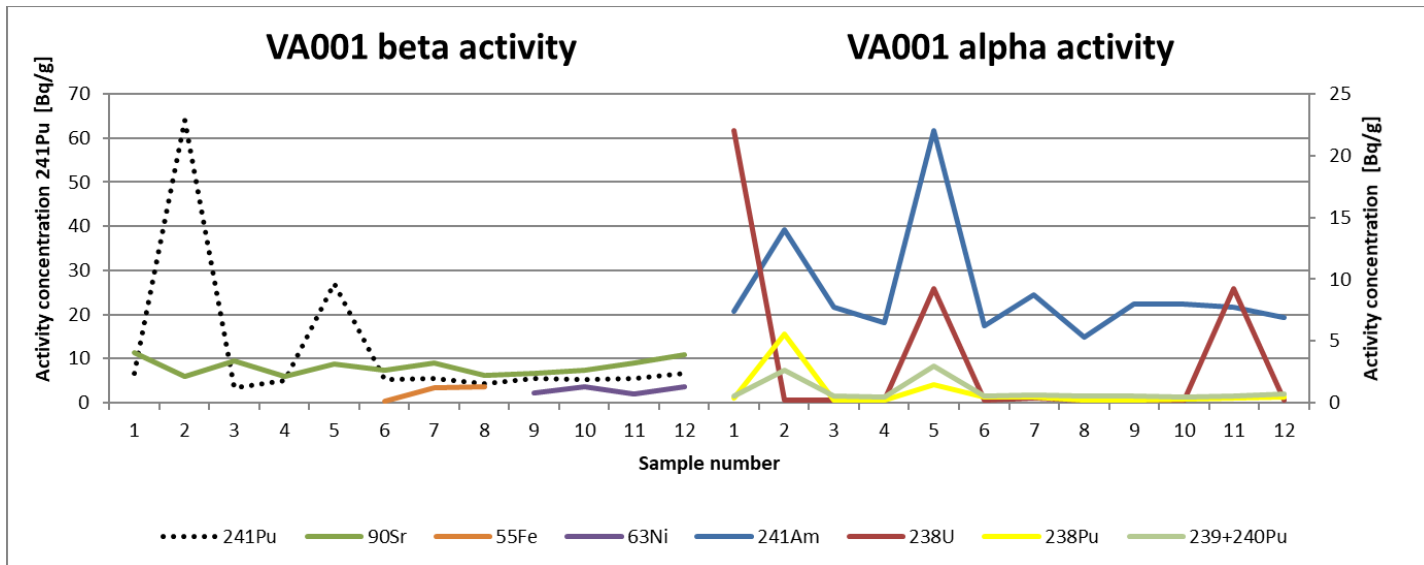


Figure 2: Radionuclide analysis (tank VA001): beta and alpha activity concentration (primary axis: ^{241}Pu , secondary axis: all other nuclides)

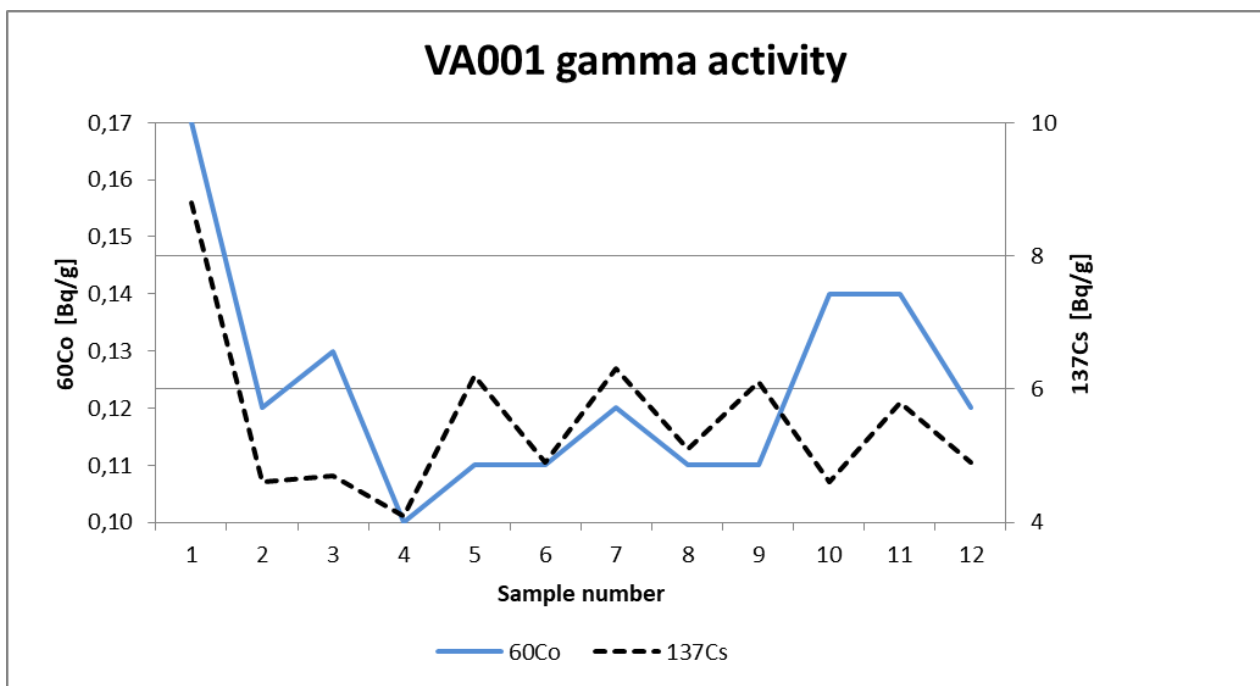


Figure 3: Radionuclide analysis (tank VA001): gamma activity concentration

For this tank, eight radionuclides have been detected on all twelve samples, i.e. ^{60}Co , ^{90}Sr , ^{137}Cs , ^{241}Pu , ^{238}Pu , ^{238}U , $^{239+240}\text{Pu}$ and ^{241}Am and for the two radionuclides ^{55}Fe and ^{63}Ni , we have some valid measurements and some limit of detection measurements. All the valid measurements are associated to uncertainties.

In Figure 4, we can see the histograms for the completely detected radionuclides. The dispersion of these data is mostly asymmetrical and the variation range is more significant for ^{137}Cs , ^{241}Pu , and ^{241}Am .

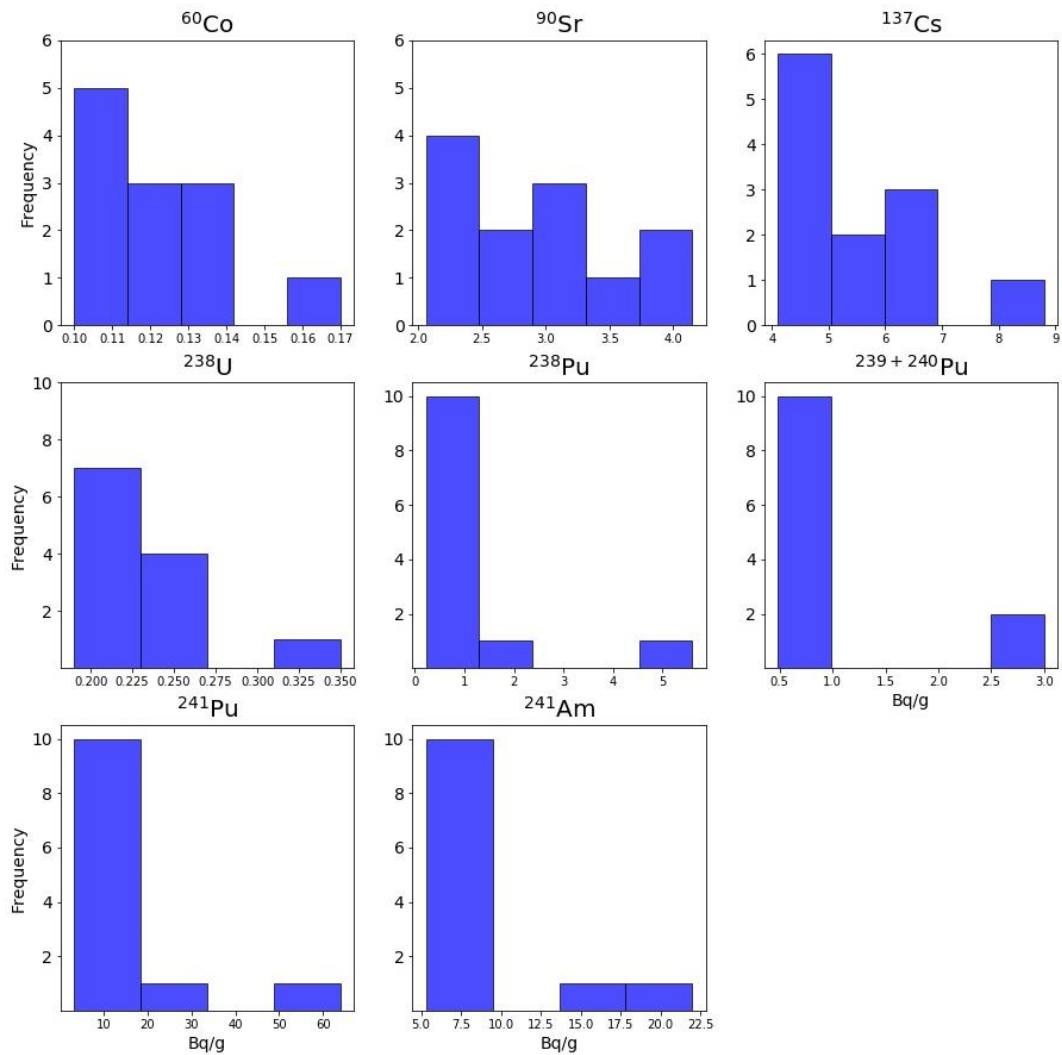


Figure 4: Histograms for the eight completely measured radionuclides in tank VA001 (status 2012).

In Figure 5, the boxplots complete the graphical exploratory analysis. Here, the boxplots diagrams, produced by using the python routine matplotlib, are based on boxes from the first to the third quartile of the data with a line at the median. The whiskers are placed by default at a distance of 1.5 times the interquartile range from the box – anything outside this range is considered an outlier. In the figure, we observe significant outliers for ^{241}Pu , ^{238}Pu , ^{238}U and $^{239+240}\text{Pu}$, circled in red in the figure.

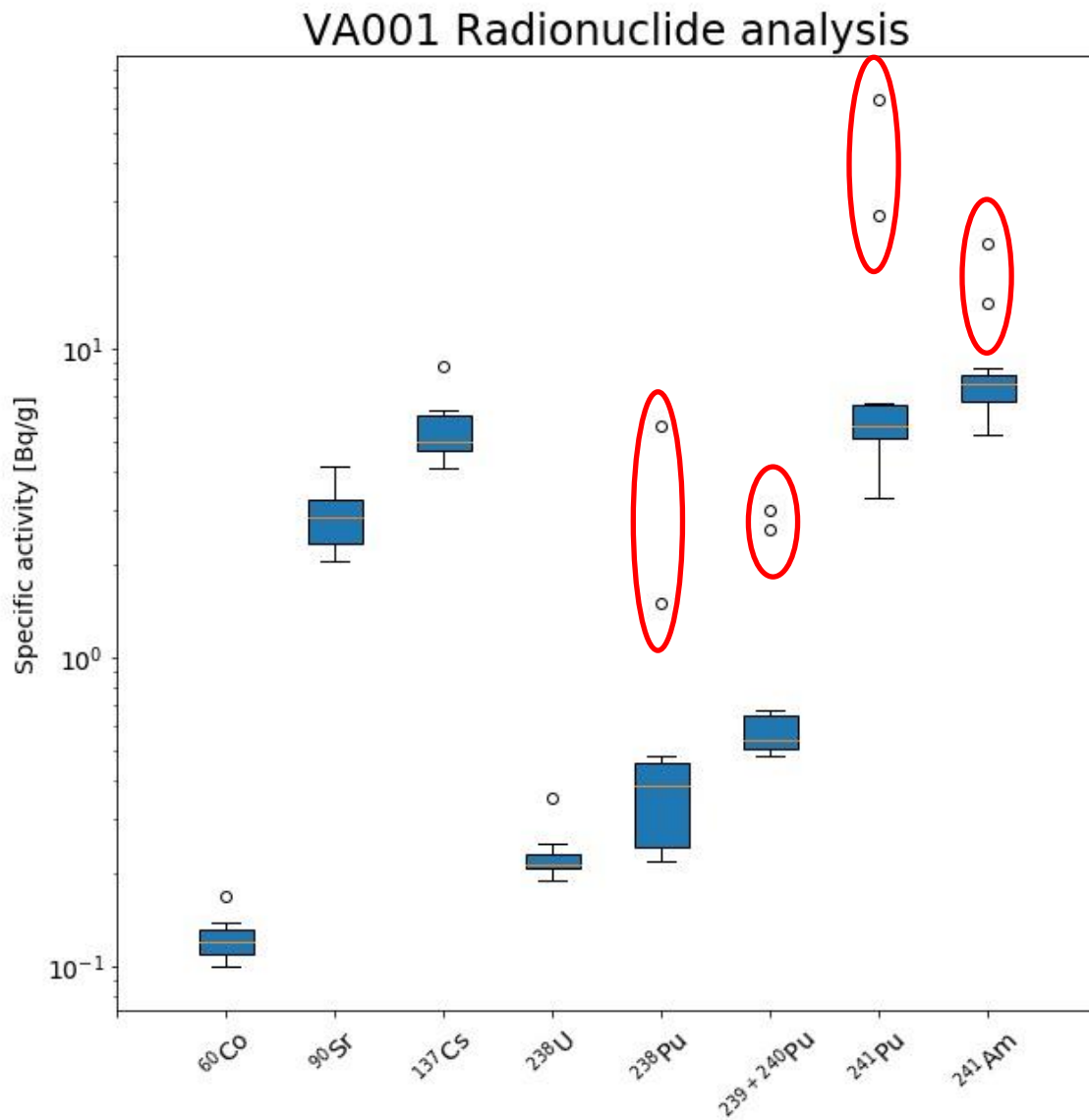


Figure 5: Boxplots for the eight completely measured radionuclides in tank VA001 (status 2012).

There are some significant linear correlations as we can see in Figure 6, i.e. between ^{60}Co and ^{60}Sr , ^{60}Co and ^{137}Cs , ^{137}Cs and ^{90}Sr , ^{137}Cs and ^{238}U and between the Pu-nuclides ^{241}Pu , ^{238}Pu , and $^{239+240}\text{Pu}$, and ^{241}Am respectively. It is also clear from the figure that the correlations between the Pu-isotopes and ^{241}Am are likely an artefact of the outliers in their data.

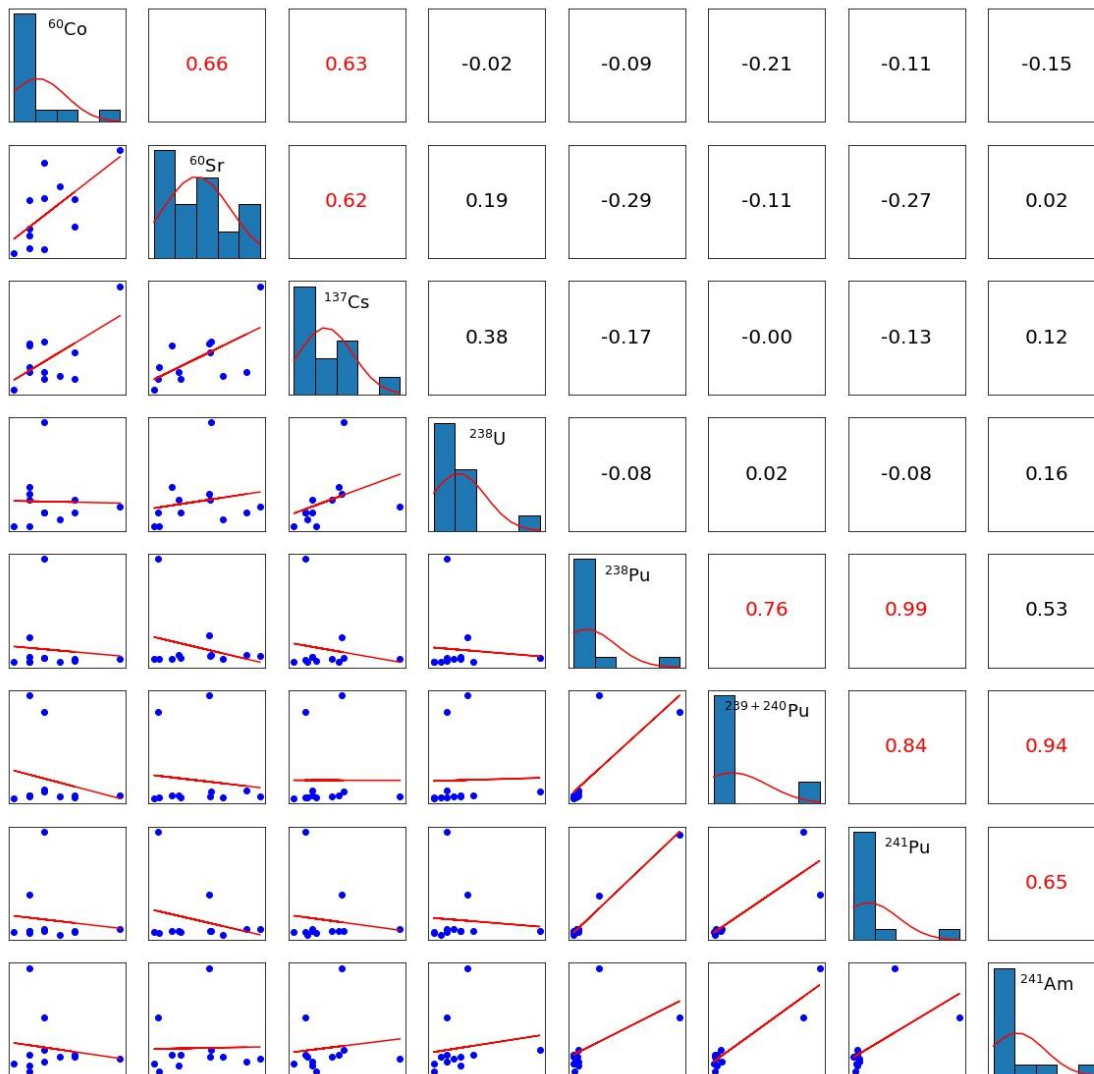


Figure 6: Linear correlations between the eight completely detected radionuclides in tank VA001, linear scale (status: 2012).

To check if the correlations are the result of outliers, we have removed these and recalculated the correlations, as shown in Figure 7. This confirms the suspicion that in all but one case the correlations observed previously are the result of outliers being present.

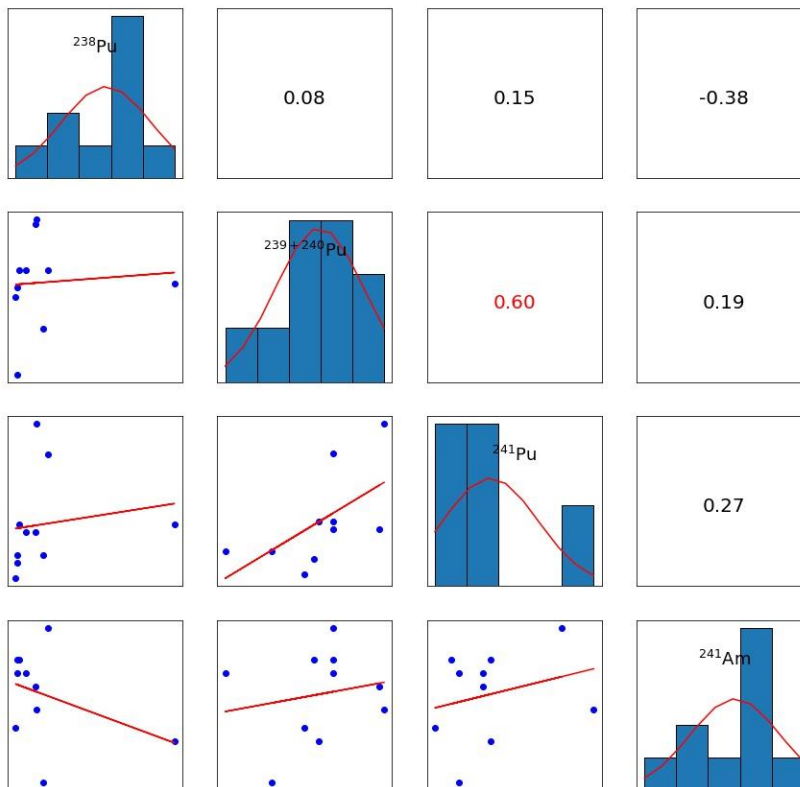


Figure 7: Linear correlations with outliers removed, tank VA001, status 2012.

In Figure 8, we present the correlation circle for the projection of radionuclide activity variables on the first two principal components of PCA analysis. Data variability is well represented by the first two components that summarize more than 70% of the total inertia. Moreover, the graph shows two multilinear correlation clusters: one contains ^{90}Sr , ^{60}Co , ^{238}U and ^{137}Cs and another contains ^{238}Pu , ^{241}Pu and $^{239+240}\text{Pu}$.

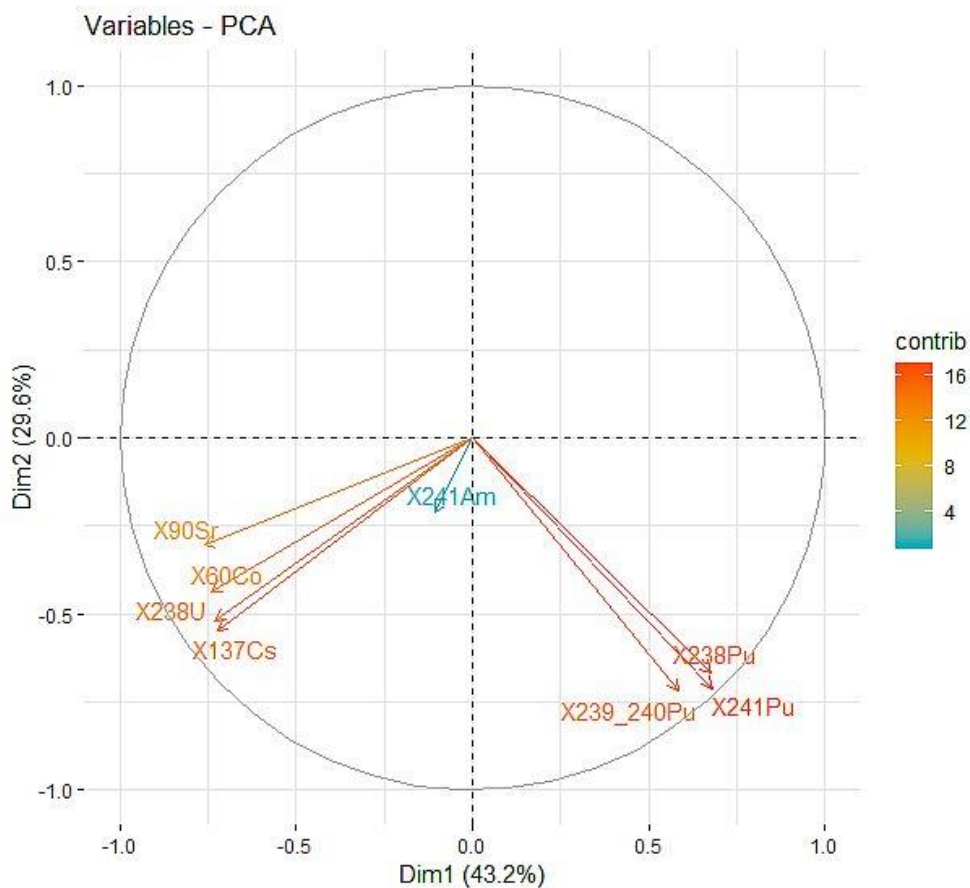


Figure 8: Variable projection on the first two principal components for radionuclide activities of VA001.

2.2.2 Tank VA002

The radioactivity content of tank VA002 was of similar magnitude as that of tank VA001, with activities of a few Bq/g for radionuclides detected, but in any case not far exceeding 100 Bq/g for the highest activity concentration (¹³⁷Cs). A summary is shown in Figure 9 (beta and alpha activity) and Figure 10 (gamma activity), with relative activities by nuclide between the two tanks ranging between the same order of magnitude and a factor of up to 25.

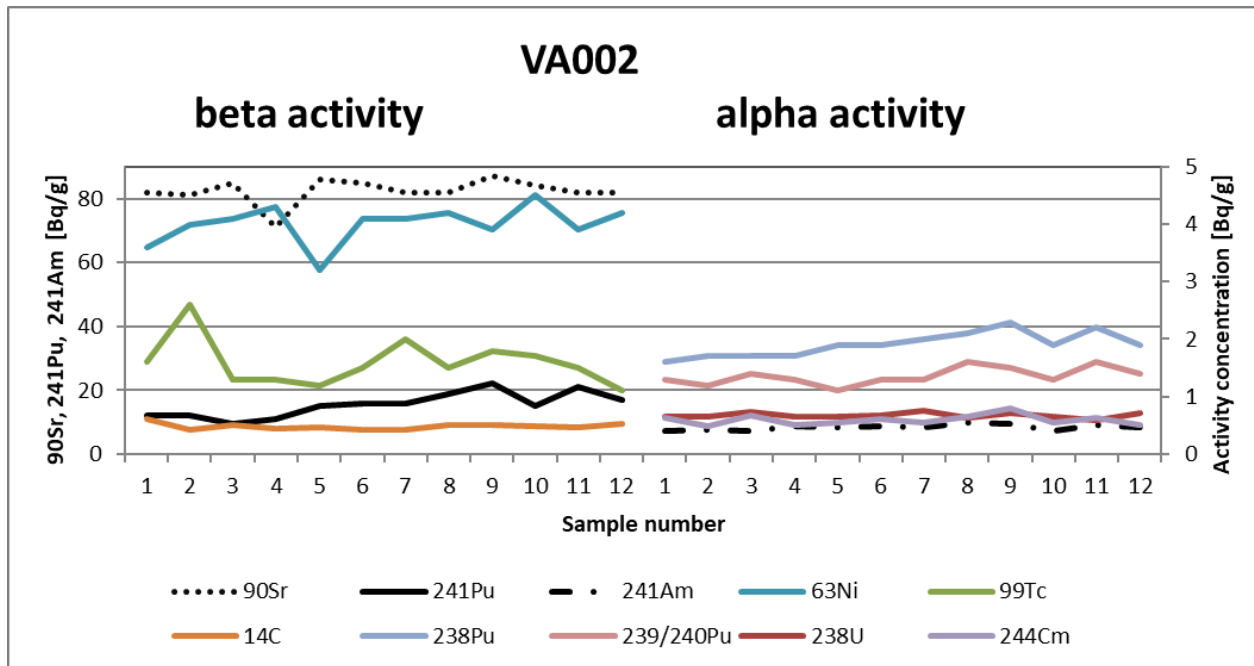


Figure 9: Radionuclide analysis (tank VA002, status 2013): beta and alpha activity concentration (primary axis: ^{90}Sr , ^{241}Pu and ^{241}Am , secondary axis: all remaining nuclides)

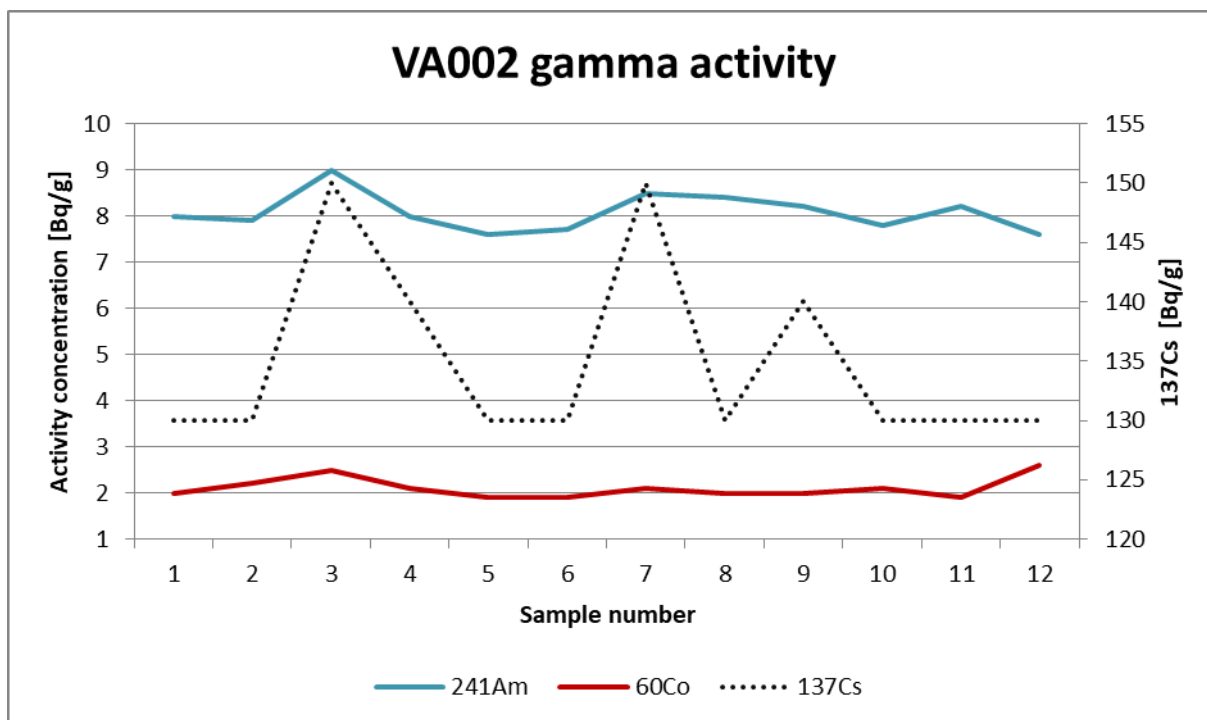


Figure 10: Radionuclide analysis (tank VA002, status 2013): gamma activity concentration (secondary axis: ^{137}Cs)

The radionuclides completely detected and analyzed here are ^{14}C , ^{60}Co , ^{63}Ni , ^{90}Sr , ^{99}Tc , ^{137}Cs , ^{238}U , ^{238}Pu , ^{241}Pu , $^{239+240}\text{Pu}$, ^{241}Am , ^{244}Cm . In

Figure 11, we show the histograms for the completely measured radionuclides and in Figure 12 the boxplots complete the graphical descriptive analysis. The dispersion of these data is mostly

asymmetrical and variation range is more significant for ^{137}Cs , ^{90}Sr and ^{241}Pu . Unlike what we observed for tank VA001, there are no significant outliers.

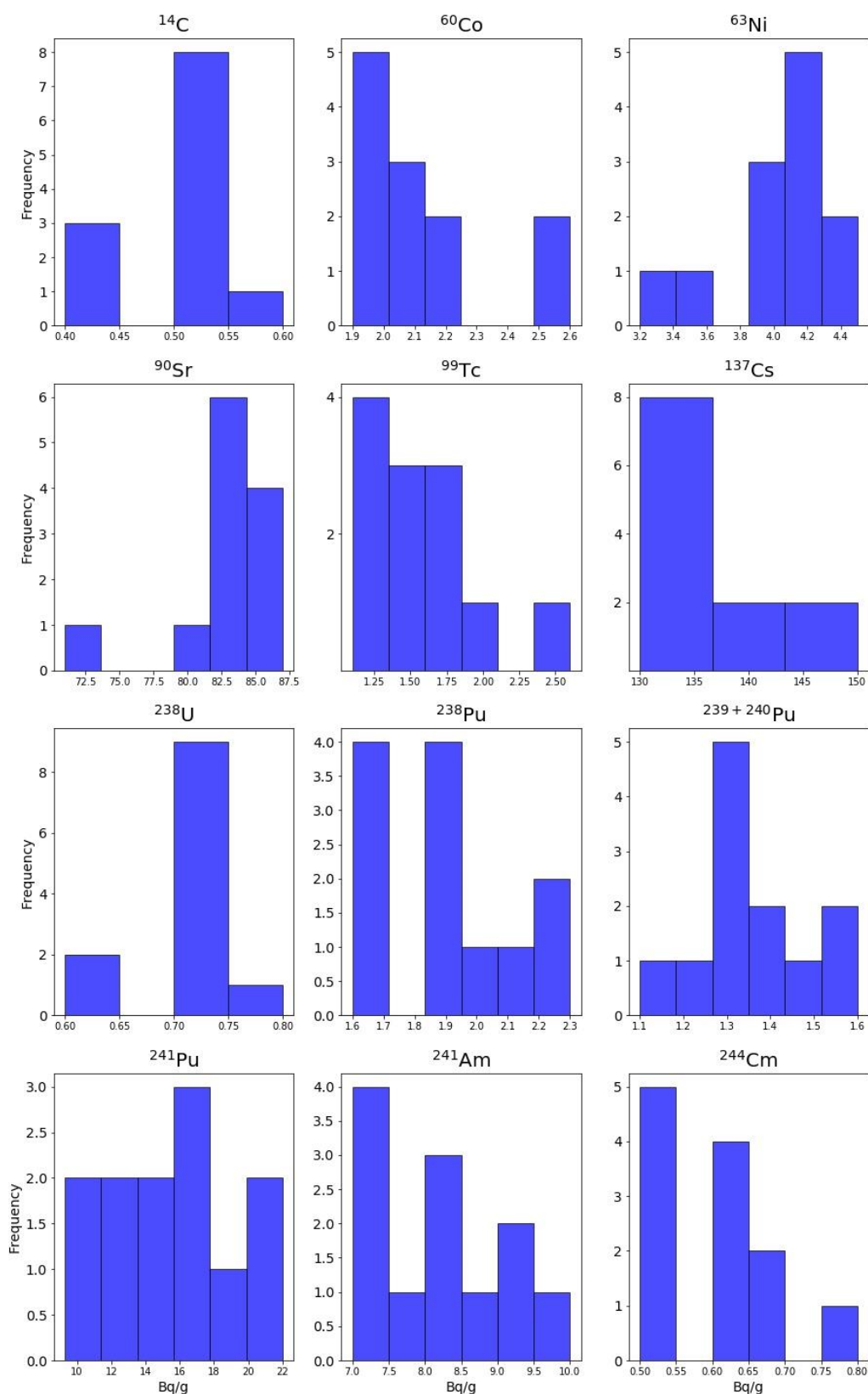


Figure 11: Histograms for the measured radionuclides in tank VA002 (2013).

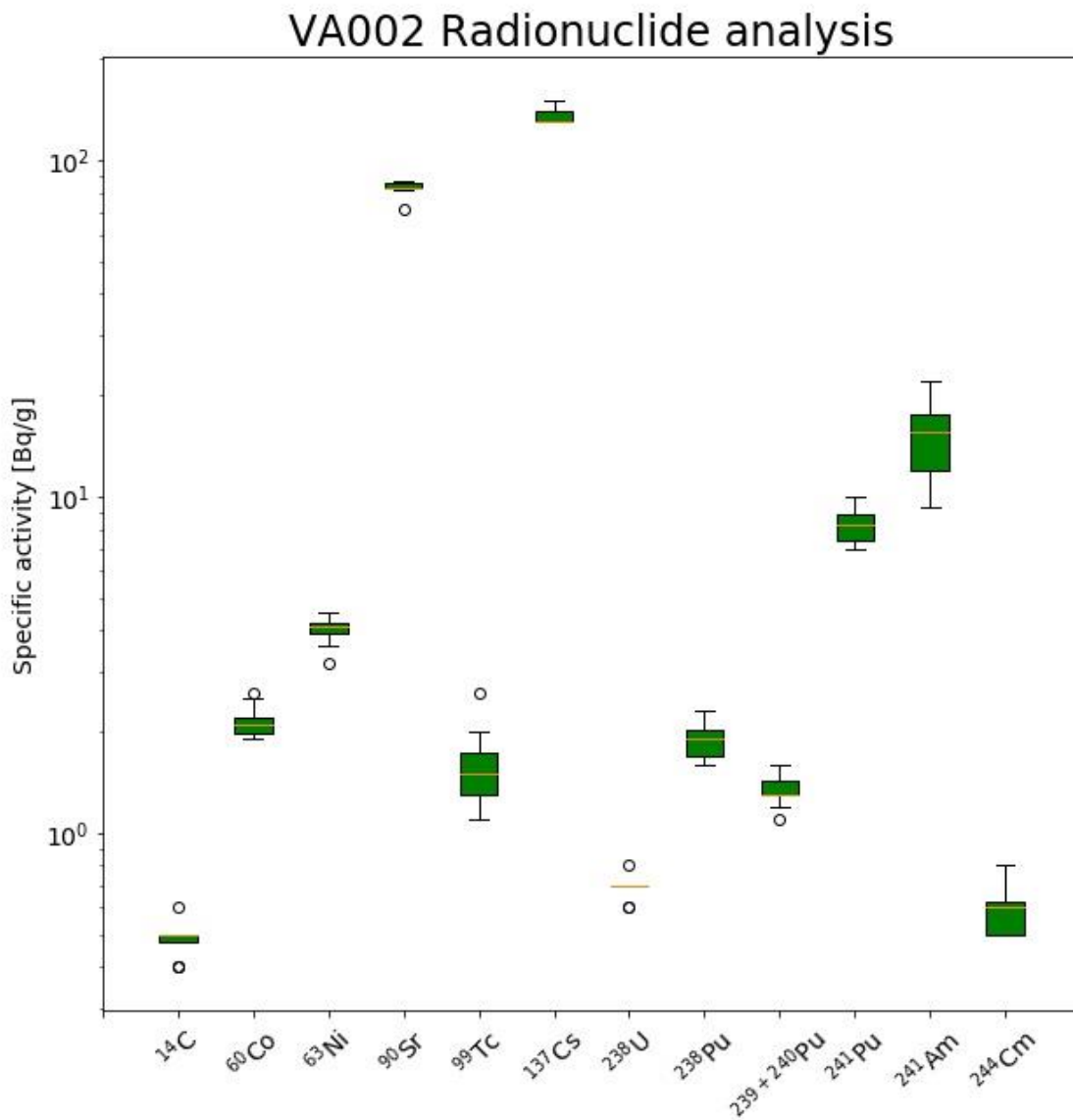


Figure 12: Boxplot for the measured radionuclides in tank VA002 (2013).

As shown in Figure 13, in which the Pearson's correlation coefficient between nuclides is summarised, there are only relevant correlations between ¹³⁷Cs with ²³⁸U, as well as between Pu-nuclides.

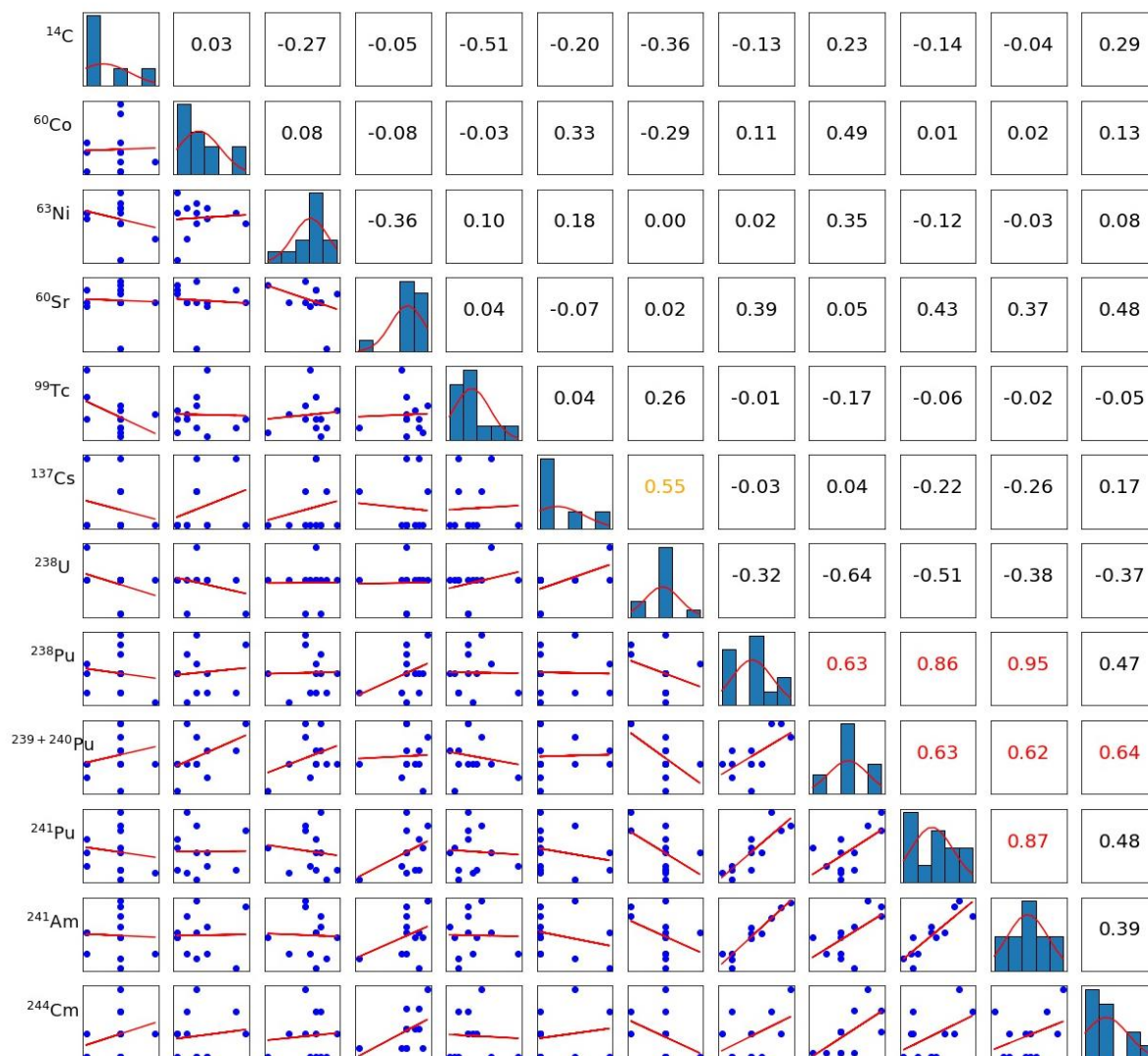


Figure 13: Linear correlations between the measured radionuclides in tank VA002.

In Figure 14, we present the correlation circle for the projection of radionuclide activity variables on the first two principal components of PCA analysis. Data variability is represented well by the first two components that summarize almost 50% of the total inertia. Nevertheless, that graph does not show multilinear correlation clusters but only linear correlations between ^{137}Cs and ^{241}Am , ^{241}Pu and ^{238}Pu , $^{239+240}\text{Pu}$ and ^{244}Cm , as have already been identified in Figure 13. Variable projection on components 2 and 3 does not give more information.

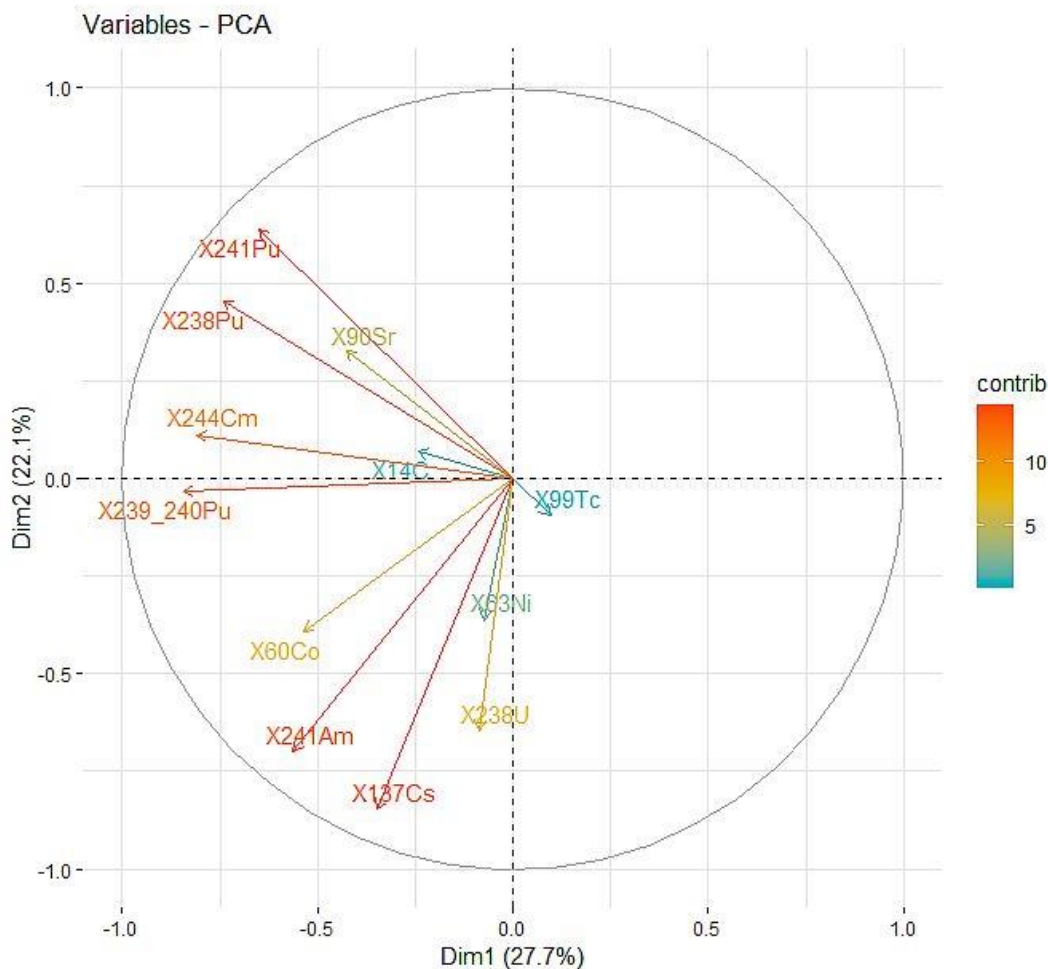


Figure 14: Variable projection on the first two principal components for radionuclide activities of tank VA002.

2.2.3 Conclusion on the exploratory data analysis

Initial inspection of the data has revealed some **outliers** in tank VA001, which cannot a priori be explained as errors, while outliers in tank VA002 were not observed.

The data set presents a **univariate** situation as the objective is to determine the total activity for each tank. Distribution of radioactivity in the tanks is expected to display a spatial trend, after settling has occurred. However, the existing samples were collected shortly after the tanks were filled while circulating the contents of the tank. Therefore, for this original data we expect **no spatial structure**. We only noticed a few linear correlations between some radionuclides and two multilinear correlation clusters for tank VA001. We observe no such trends in tank V002. Since the data sets are small, **robust methods** for inference will be beneficial according to the INSIDER data analysis and sampling design strategy.



2.3 Data analysis

There are two tanks to characterize, i.e. VA001 and VA002, and for each one the identified radionuclides are different. We performed the same statistical methodology on each of the two tanks in order to quantify the activity of each radionuclide and we show the benefits provided by taking into account measurement uncertainties and limit of detection to obtain estimations that are more realistic.

2.3.1 Tank VA001

As we study small data sets of sample size twelve, it is important to assess the representativeness of these data. For that, as explained in ([Pérot, N. et al. 2017](#)), we perform bootstrap estimations of mean and standard deviation with their confidence interval, using a resampling strategy based on replicates size ranging from 5 to 12. In Figure 15, the graphs show the evolution of mean bootstrap estimations and confidence intervals. In each case, the bottom orange line represents the lowest estimate of the mean and the top blue line the maximum for the estimate for each simulation. For ^{60}Co , ^{90}Sr , ^{137}Cs and ^{241}Am , the points show a regular stability of the estimations and a decrease of the confidence interval width, which seems to reach stabilization at a sample size of about 10. These elements contribute to deduce the representativeness of the measurement data sets for each of these radionuclides. The results for the standard deviation are very similar. Nevertheless, the results for ^{241}Pu , ^{238}Pu , ^{241}Pu and $^{239+240}\text{Pu}$ are not of the same type. For these radionuclides, the upper bound of the confidence interval is very irregular, which can be explained by the outliers identified (circled in red) in the boxplot graphs (Figure 5).

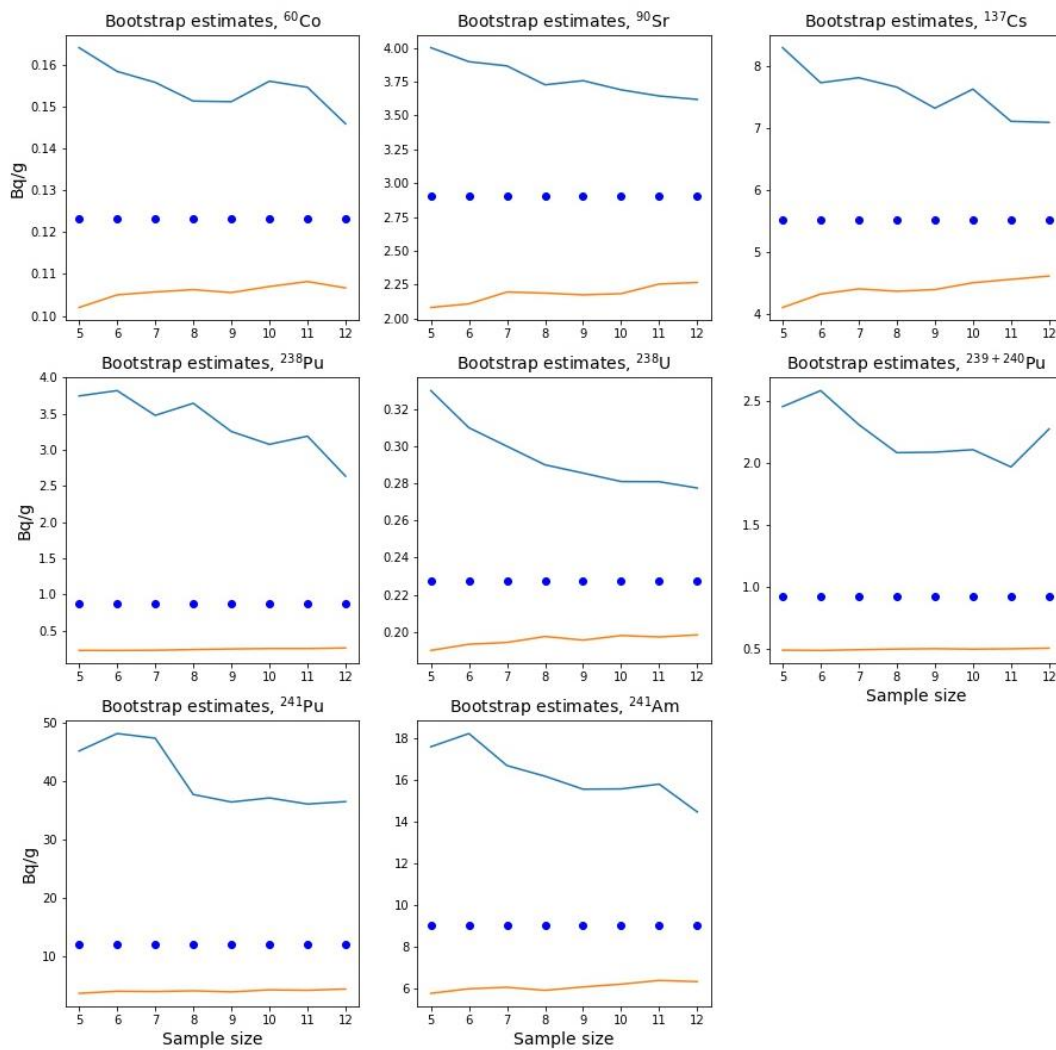


Figure 15: Mean bootstrap estimation as a function of the number of replicates for the eight measured radionuclides in tank VA001 (status 2012).

In Figure 16, the graphs on the left show the evolution of the mean bootstrap estimations and confidence intervals for ^{241}Pu , ^{238}Pu , ^{238}Pu and $^{239+240}\text{Pu}$, including outliers. The graphs on the right show the bootstrap results without taking into account outliers. These last results are more regular and as for the other radionuclides give confidence on representativeness of the corresponding measurement data sets.

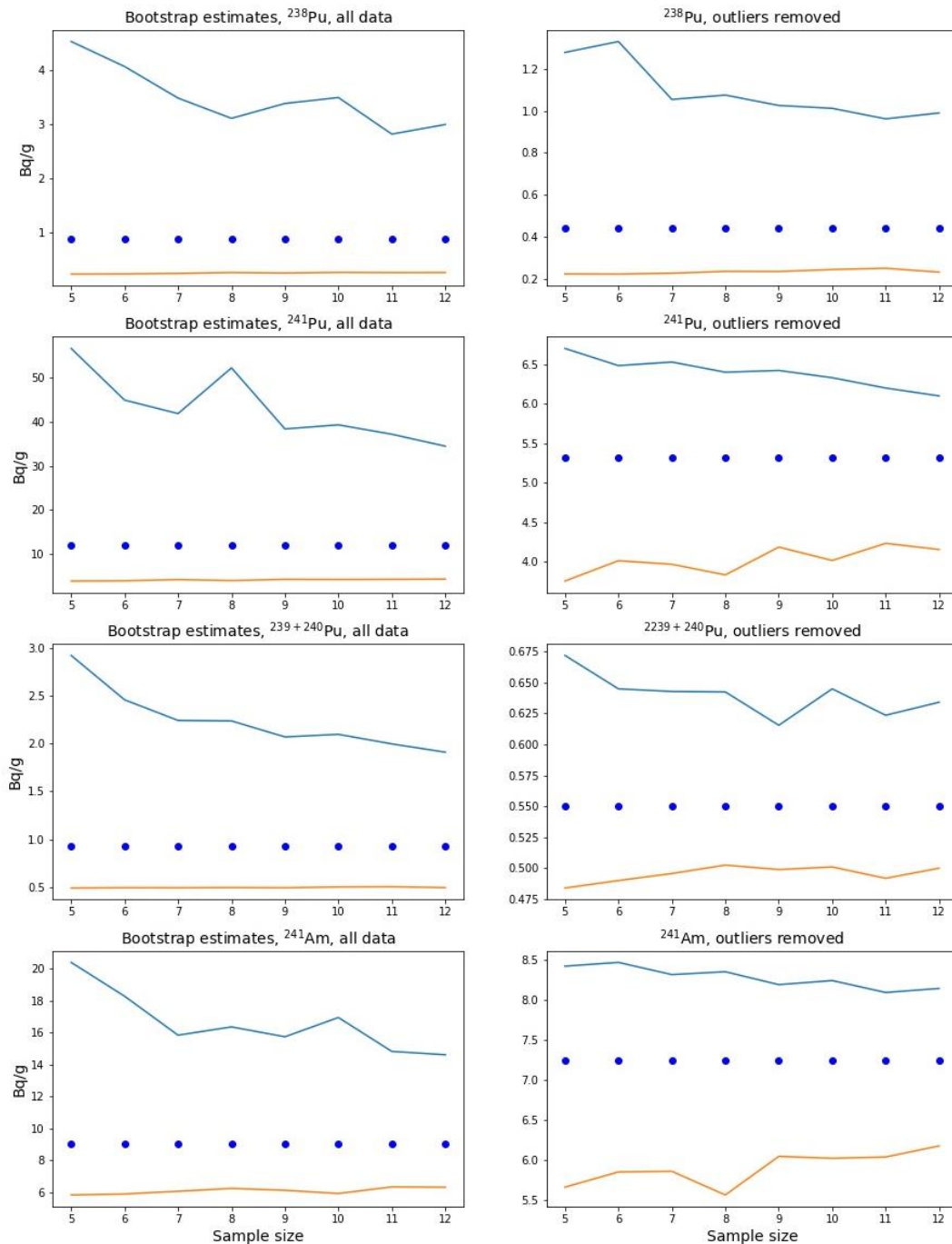


Figure 16: Mean bootstrap estimation as a function of the number of replicates for ^{241}Pu , ^{238}Pu , $^{239+240}\text{Pu}$ and ^{241}Am in tank VA001 with (left) and without outliers (right).

For the next step, we perform probabilistic law fitting on data measurements for the ten radionuclides ^{60}Co , ^{90}Sr , ^{137}Cs , ^{241}Pu , ^{238}Pu , ^{238}U , $^{239+240}\text{Pu}$, ^{241}Am , ^{55}Fe and ^{63}Ni , taking into account uncertainties and limit of detection of measurements but excluding outliers. The radionuclides not found to be present in activities exceeding detection limits are omitted from this analysis, as their activities conceivably are so low that they will automatically satisfy the WAC without further inspection.

Uncertainties and limits of detection are used as incomplete information that help the estimation to be more realistic. In Table 4, we show estimations of the mean provided by the different methods

described in (Pérot, N. et al, 2017), for each of the radionuclides: empirical mean, Wilks median, bootstrap estimation of mean, Bayesian estimation, mean estimated from fitted theoretical distribution law on data without uncertainties and limits of detection, mean estimated from fitted theoretical distribution law on data with uncertainties and limits of detection, provided by the CARTOSTAT0D software. The differences between the estimations from theoretical probabilistic laws fitted without uncertainties and limit of detection (limit of detection are considered as valid data here) and from theoretical probabilistic laws fitted with a specific treatment of uncertainties and limits of detection can be important. For five radionuclides, the estimations provided by CARTOSTAT0D methodology are between 10% and 47% lower and particularly for radionuclides with limit of detection measurements, i.e. ^{55}Fe and ^{63}Ni .

Table 4: Mean estimations with the different methods for the completely measured radionuclides and for radionuclides with limit of detection measurements in tank VA001.

Radionuclide	Empirical mean	Wilks median (50%, 98%, 3rd)	Bootstrap estimate	Bayesian estimation	Theoretical mean without uncertainty	Theoretical mean with uncertainty CARTOSTAD0D	Difference between with and without uncertainty
	Bq/g	Bq/g	Bq/g	Bq/g	Bq/g	Bq/g	%
^{60}Co	0.12	0.14	0.12	0.12	0.13	0.12	-8
^{90}Sr	2.9	3.4	2.9	2.9	2.7	3.1	14
^{137}Cs	5.5	6.2	5.5	5.5	5.8	5.1	-11
^{241}Pu	12.0	6.7	10	5.2	5.3	5.6	6
^{238}Pu	0.9	0.5	0.9	0.7	0.34	0.5	47
^{238}U	2.0	0.3	2	0.7	0.24	0.21	-13
$^{239+240}\text{Pu}$	0.9	0.7	0.9	0.8	0.56	0.57	2
^{241}Am	8	8	8.0	8.1	6.4	9.0	41
$^{55}\text{Fe}^*$	0.8	1.2	-	1.0	0.9	0.5	-47
$^{63}\text{Ni}^*$	0.7	1.3	-	0.7	0.7	0.5	-29

In Table 5, we show 90%-quantile estimations provided by the different methods described in (Pérot, N. et al, 2017), for each of the radionuclides. For six radionuclides, the estimations provided by the CARTOSTAT0D methodology are between 7% and 49% lower than the theoretical predictions, particularly so for radionuclides with limit of detection measurements, i.e. ^{55}Fe and ^{63}Ni . Figure 17 shows a graphical representation of these results.

Table 5: 90%-quantile estimations with the different methods for the completely measured radionuclides and for radionuclides with limit of detection measurements in tank VA001.

Radionuclide	Empirical mean	Wilks quantile (80%, 92%)	Bootstrap estimate	Bayesian estimation	Theoretical mean without uncertainty	Theoretical mean with uncertainty CARTOSTADOD	Difference between with and without uncertainty
	Bq/g	Bq/g	Bq/g	Bq/g	Bq/g	Bq/g	%
⁶⁰ Co	0.14	0.17	0.14	0.14	0.14	0.13	-7
⁹⁰ Sr	3.9	4.1	3.7	3.8	3.2	3.6	12
¹³⁷ Cs	6.3	8.8	6.8	6.9	6.6	5.9	-11
²⁴¹ Pu	25.0	64	27	21	6.5	6.4	-1
²³⁸ Pu	1.4	5.6	2	1.5	0.5	0.7	40
²³⁸ U	0.3	22	5.5	1.7	0.3	0.3	-11
²³⁹⁺²⁴⁰ Pu	2.4	3	1.9	1.6	0.6	0.7	6
²⁴¹ Am	8.6	22	11.6	14.5	10.5	14.7	40
⁵⁵ Fe*	1.3	3.9	-	2.2	2.1	1.1	-49
⁶³ Ni*	1.3	1.6	-	1.3	1.3	0.9	-28

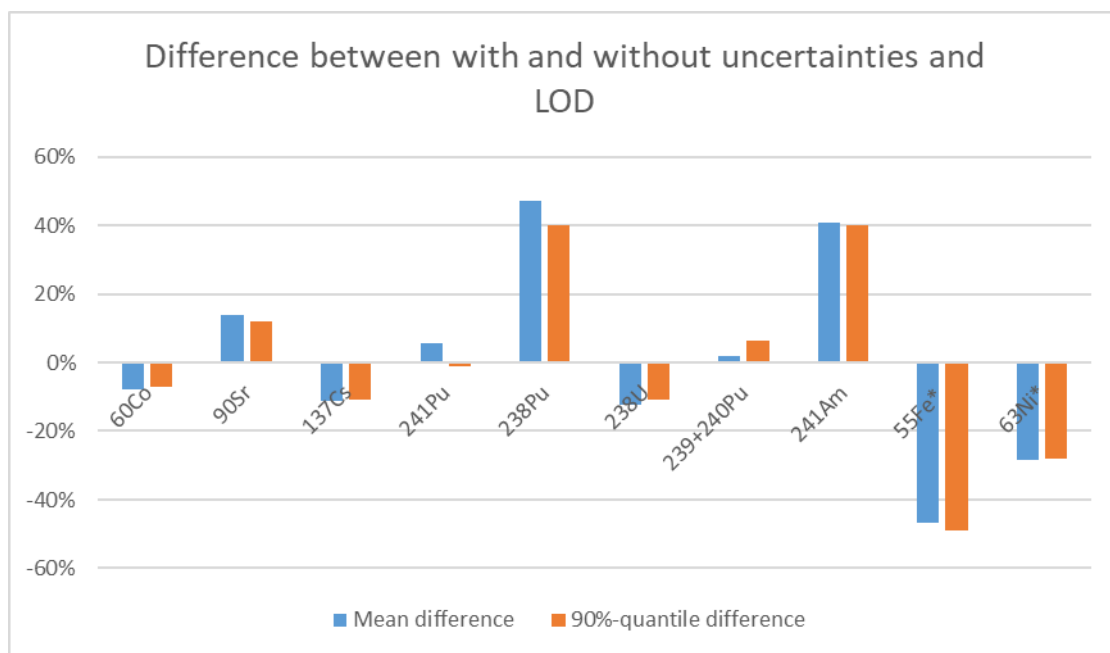


Figure 17: Difference between estimations with and without uncertainties and limit of detection specific treatment for radionuclide activities in tank VA001.

Figure 18 shows the mean estimations for each radionuclide for all the methods performed. As expected, empirical, Wilks and bootstrap estimations are more conservative for radionuclides with outliers compared to the other methods.

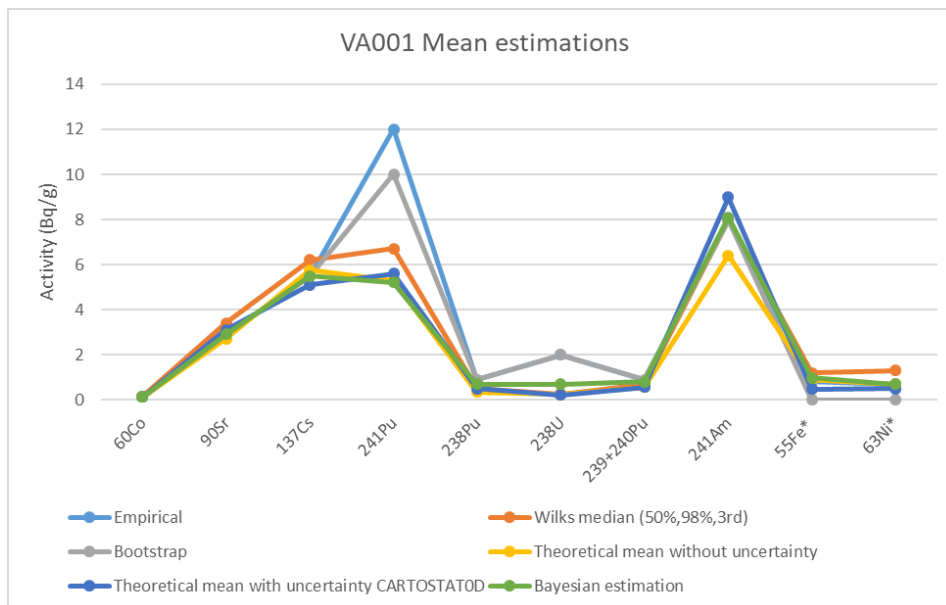


Figure 18: Mean estimations with the different methods for radionuclide activities in VA001 tank.

Figure 19 shows the 90%-quantile estimations for each radionuclide and for all the methods performed. As expected, Wilks estimations are often the most conservative (is the maximum of the sample then the maximum of the outliers). We also observe conservative results for bootstrap estimations for radionuclides with outliers.

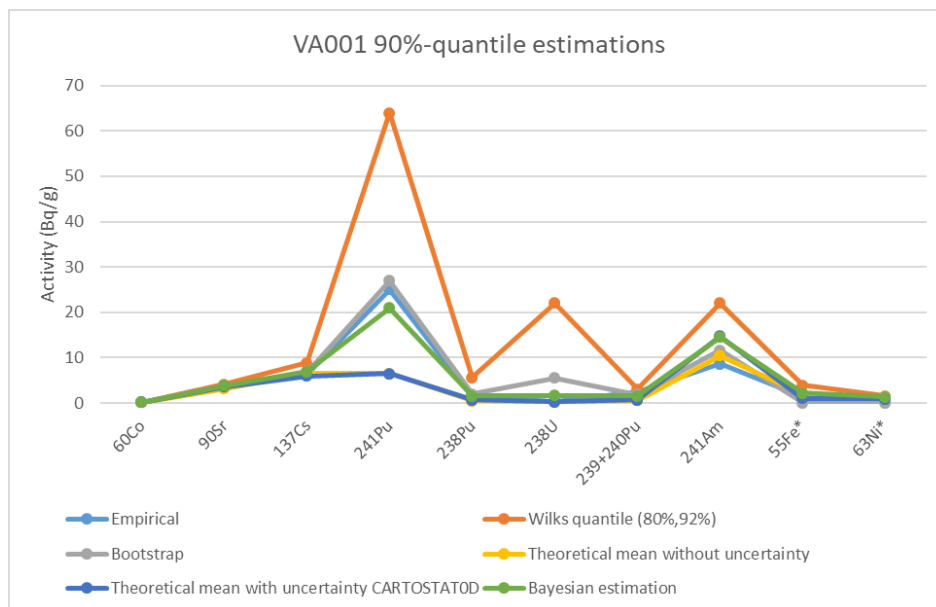


Figure 19: 90%-quantile estimations with the different methods for radionuclide activities in VA001 tank.

In the next step, we perform the methodology called probabilistic risk bound described in ([Blatman, G. et al 2017](#)) that is very useful for risk analysis. With this method, if the data satisfy some hypothesis like the unimodality or the convexity of the probabilistic distribution tail, we can use Camp-Meidel or Van Danzig inequality and estimate the probability to exceed a given threshold. For this study, all

the radionuclide data measurements satisfy the hypothesis of the probabilistic distribution tail convexity, so we perform the Van Dantzig inequality to estimate the probabilities $P(X > S)$ to exceed two given threshold S of 10 Bq/g and 100 Bq/g with the empirical estimations of mean and standard deviation. We also estimate the probability $P(X > S)$ from the fitted distribution laws with and without taking into account uncertainties and limits of detection.

Inspection of the WAC in Table 3 confirms that the maximum specific activities specified in the WAC are far larger than any of the specific activities detected in the lab analysis. Nevertheless, for purposes of demonstration only, we display results from the probabilistic risk bound for exceeding the threshold of 10 Bq/g and 100 Bq/g respectively.

As we can see in Table 6, the estimations provided by the probabilistic risk bound method are more conservative but certainly more robust when we consider that the probabilistic distributions have been fitted on a small data set of size twelve.

Table 6: Estimation of probabilities to exceed two given thresholds with probabilistic risk bound method and with fitted theoretical distribution laws for radionuclide activities of tank VA001.

Threshold [Bq/g]	Probabilistic risk bound		Theoretical law without uncertainties + LOD		Theoretical law with uncertainties + LOD	
	10	100	10	100	10	100
	Probability to exceed threshold [%]					
⁶⁰ Co	1.40E-04	1.30E-06	0.00E+00	0.00E+00	0.00E+00	0.00E+00
⁹⁰ Sr	3.40E-01	1.80E-03	7.00E-07	0.00E+00	7.00E-11	0.00E+00
¹³⁷ Cs	2.90E+00	6.70E-03	9.00E-02	0.00E+00	1.70E-02	0.00E+00
²⁴¹ Pu	9.70E+01	1.50E+00	4.30E-05	0.00E+00	2.00E-04	0.00E+00
²³⁸ Pu	1.00E+00	9.00E-03	0.00E+00	0.00E+00	0.00E+00	0.00E+00
²³⁸ U	1.90E+01	1.50E-01	0.00E+00	0.00E+00	0.00E+00	0.00E+00
²³⁹⁺²⁴⁰ Pu	3.50E-01	3.00E-03	0.00E+00	0.00E+00	0.00E+00	0.00E+00
²⁴¹ Am	1.30E+01	2.30E-02	5.00E+00	0.00E+00	4.00E+00	0.00E+00
⁵⁵ Fe	5.00E-01	4.00E-03	7.00E-03	1.00E-14	1.50E-02	1.00E-07
⁶³ Ni	9.00E-02	8.00E-04	1.00E-04	0.00E+00	7.00E-09	0.00E+00

For objectives of categorization with thresholds prescribed by regulatory framework, these methods and results are of main importance and constitute meaningful inputs for the development of D&D scenarios.

2.3.2 Tank VA002

In order to assess the representativeness of these data and as explained in ([Pérot, N. et al, 2017](#)), we perform bootstrap estimations of mean and standard deviation with their confidence interval with a resampling strategy based on replicates ranging from size 5 to 12. In Figure 20, the graphs show the evolution of mean bootstrap estimations. We note a regular stability of the estimations and a decrease of the confidence interval width, which seems to reach stabilization at a size of about 10

data points. These elements contribute to deduce the representativeness of the measurement samples for each radionuclide. The results for the standard deviation are very similar except for ^{137}Cs for which the lower bound of the confidence interval is less regular.

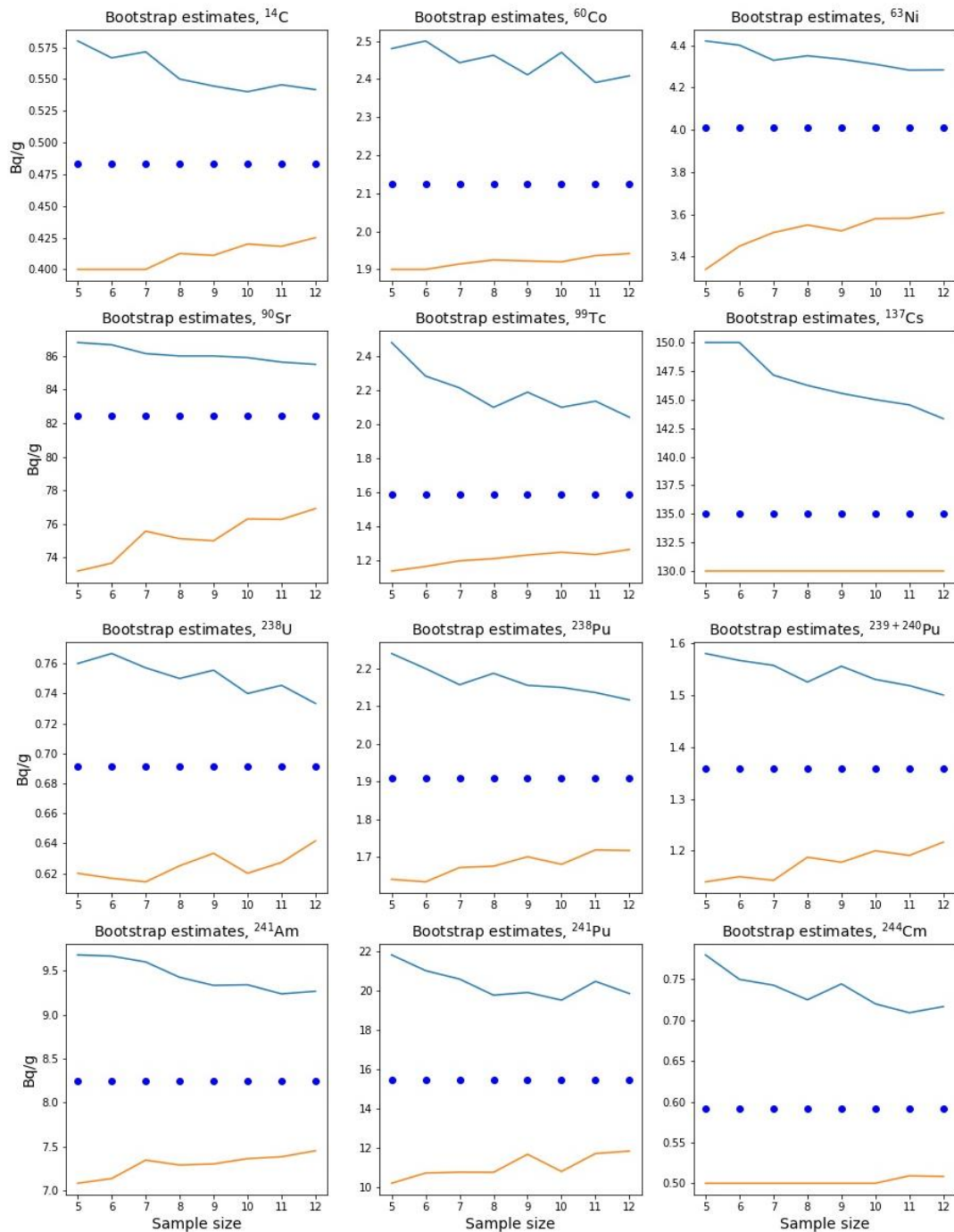


Figure 20: Mean bootstrap estimation varying with the size of the replicates for the measured radionuclides in tank VA002.

For the next step, we perform probabilistic law fitting on data measurements for the eleven radionuclides ^{14}C , ^{60}Co , ^{63}Ni , ^{90}Sr , ^{99}Tc , ^{137}Cs , ^{238}U , ^{238}Pu , ^{241}Pu , ^{241}Am , $^{239+240}\text{Pu}$ and ^{244}Cm , taking into account uncertainties.

The results presented here have been provided by CARTOSTAT-0D. In this case, we have uncertainties that are used as incomplete information that help the estimation to be more realistic. In Table 7, we show mean estimations provided by different methods described in (Pérot, N. et al, 2017) and for each radionuclide. The differences can be important between the estimations from theoretical probabilistic laws fitted without uncertainties and from theoretical probabilistic laws fitted with a specific treatment of uncertainties. For ²⁴¹Pu, the estimation provided by CARTOSTAT0D methodology is 13% lower and for the other radionuclides, the estimations are up to 20% higher. The results obtained for 90%-quantile estimations shown in

Table 8 are very similar. Figure 21 shows a graphical representation of these results.

Table 7: Mean estimations with the different methods for the measured radionuclides in VA002 tank.

Radionuclide	Empirical mean	Wilks median (50%, 98%, 3rd)	Bootstrap estimate	Bayesian estimation	Theoretical mean without uncertainty	Theoretical mean with uncertainty CARTOSTAD0D	Difference between with and without uncertainty
	Bq/g	Bq/g	Bq/g	Bq/g	Bq/g	Bq/g	%
¹⁴ C	0.48	0.5	0.48	0.48	0.5	0.5	0
⁶⁰ Co	2.1	2.2	2.1	2.1	2	2.2	10
⁶³ Ni	4	4.2	4.01	4.01	4.1	4.1	0
⁹⁰ Sr	82.4	85	82	82.4	81	83	2
⁹⁹ Tc	1.6	1.8	1.6	1.6	1.7	1.7	0
¹³⁷ Cs	135	140	135	135	133	137	3
²³⁸ U	0.67	0.7	0.67	0.67	0.67	0.68	1
²³⁸ Pu	1.9	2.1	1.9	1.9	1.9	2	5
²⁴¹ Pu	15	19	15	15	16	14	-13
²³⁹⁺²⁴⁰ Pu	1.3	1.4	1.3	1.3	1.3	1.4	8
²⁴¹ Am	8.1	8.4	8.1	8.1	8.2	8.2	0
²⁴⁴ Cm	0.6	0.7	0.6	0.6	0.5	0.6	20

Table 8: 90%-quantile estimations with the different methods for the measured radionuclides in tank VA002.

Radionuclide	Empirical mean	Wilks quantile (80%, 92%)	Bootstrap estimate	Bayesian estimation	Theoretical mean without uncertainty	Theoretical mean with uncertainty CARTOSTADOD	Difference between with and without uncertainty
	Bq/g	Bq/g	Bq/g	Bq/g	Bq/g	Bq/g	%
¹⁴ C	0.52	0.6	0.53	0.54	0.54	0.57	6
⁶⁰ Co	2.5	2.6	2.4	2.4	2.3	2.4	4
⁶³ Ni	4.3	4.5	4.3	4.4	4.5	4.5	0
⁹⁰ Sr	86	87	85	88	88	88	0
⁹⁹ Tc	2	2.6	2	2.1	2.1	2.1	0
¹³⁷ Cs	149	150	145	145	141	149	6
²³⁸ U	0.74	0.75	0.72	0.73	0.7	0.73	4
²³⁸ Pu	2.2	2.3	2.1	2.2	2.2	2.3	5
²⁴¹ Pu	21	22	20	20.7	21	18	-14
²³⁹⁺²⁴⁰ Pu	1.5	1.6	1.5	1.5	1.4	1.6	14
²⁴¹ Am	8.5	9	8.5	8.6	8.6	8.8	2
²⁴⁴ Cm	0.67	0.8	0.7	0.7	0.65	0.76	17

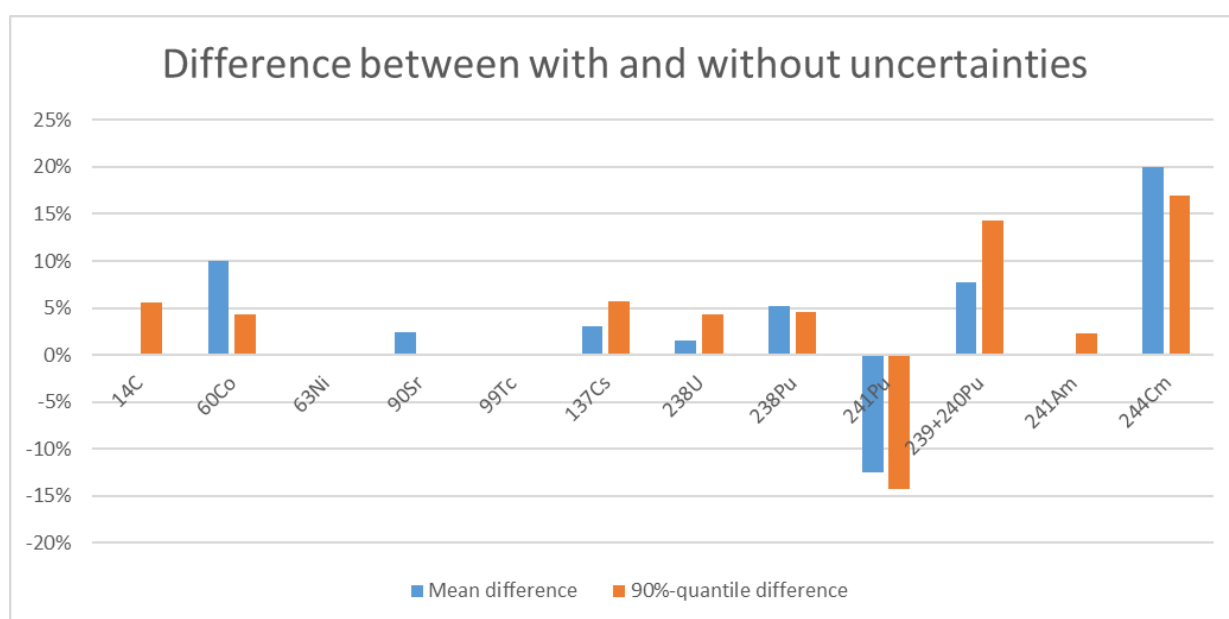


Figure 21: Difference between estimates with and without uncertainties for radionuclide activities in tank VA002.

In the next step, we perform the probabilistic risk bound method described in ([Blatman G. et al. 2017](#)). For this study, all the radionuclide data measurements satisfy the hypothesis of the probabilistic distribution tail convexity, so we perform the Van Dantzig inequality to estimate the probabilities $P(X > S)$ to exceed two given thresholds S of 10 Bq/g and 100 Bq/g with the empirical estimations of mean and standard deviation. We also estimate the probability $P(X > S)$ from the fitted distribution laws with and without taking into account uncertainties and limits of detection. As shown in Table 9, the estimations provided by the probabilistic risk bound method are more conservative but certainly more robust when we consider that the probabilistic distribution have been fitted on small data set of size twelve.

Table 9: Estimation of probabilities to exceed 2 given thresholds with probabilistic risk bound method and with fitted theoretical distribution laws for radionuclide activities of tank VA002.

Threshold [Bq/g]	Probabilistic risk bound		Theoretical law without		Theoretical law with	
	10	100	10	100	10	100
	Probability to exceed threshold [%]					
¹⁴ C	1.00E-03	9.00E-06	0.00E+00	0.00E+00	0.00E+00	0.00E+00
⁶⁰ Co	3.00E-02	2.00E-04	0.00E+00	0.00E+00	0.00E+00	0.00E+00
⁶³ Ni	1.20E-01	4.00E-04	0.00E+00	0.00E+00	0.00E+00	0.00E+00
⁹⁰ Sr	1.00E+02	2.00E+00	1.00E+02	4.00E-03	1.00E+02	1.80E-04
⁹⁹ Tc	9.00E-02	6.00E-04	1.00E-14	0.00E+00	0.00E+00	0.00E+00
¹³⁷ Cs	1.00E+02	1.00E+02	1.00E+02	1.00E+02	1.00E+02	1.00E+02
²³⁸ U	1.00E-03	8.00E-06	0.00E+00	0.00E+00	0.00E+00	0.00E+00
²³⁸ Pu	2.60E-02	2.00E-04	0.00E+00	0.00E+00	0.00E+00	0.00E+00
²⁴¹ Pu	1.60E+01	8.00E-02	9.50E+01	2.60E-12	9.50E+01	0.00E+00
²³⁹⁺²⁴⁰ Pu	8.40E-03	6.50E-05	0.00E+00	0.00E+00	0.00E+00	0.00E+00
²⁴¹ Am	1.70E+00	7.00E-04	4.00E-04	0.00E+00	3.60E-02	0.00E+00
²⁴⁴ Cm	3.50E-03	3.00E-05	0.00E+00	0.00E+00	0.00E+00	0.00E+00

2.4 Post processing: is objective achieved?

For this example, the objectives were defined artificially. Based on a total volume of roughly 50 m³ in each tank and a bulk density of 1,1 g/mL¹, the total activity per nuclide is not to exceed the maximum value defined in the WAC. As a first estimate, the exploratory analysis of the data is used to check if the criteria are met. A rough estimate of the maximum total activity per tank is to multiply the maximum specific activity determined for each nuclide with the total volume of the tanks, as summarised in Table 10 for tank VA001 and in Table 11 for tank VA002, and assuming the density

¹ Given in the pre-existing lab data for tank VA001, but not known for tank VA002.

is as determined in the chemical analysis. In addition, the activities reported in the initial data must be corrected for the time elapsed since then, about 7 years. We've chosen November 2019 for the date to compare the data, as the gamma spectrometry measurements for the on-site comparison exercises were carried out during that time (see section 3.1.2 for the discussion of the results thereof). Based on this very simple approximation, it is clear that the activity limit specified in the WAC is far larger than any of the estimates based on the maxima of the activity concentration for each nuclide. This is independent on the error margins and sensitivity analysis as the limits for the WAC are several orders of magnitude larger than the estimates of the total activity. The objective is therefore already achieved at this point in the campaign.

Table 10: Estimate of maximum total activity per nuclide, tank VA001, based on maxima measured for specific activity per nuclide and estimated total solids

	Maximum specific activity detected (2012)	WAC maximum total activity per nuclide	Estimate of maximum total activity based on maximum specific activity measured (extrapolated to November 2019)
Radionuclide	Bq/g	Bq	Bq
⁵⁵ Fe	3.9E+00	1.4E+16	2.9E+07
⁶³ Ni	1.6E+00	7.0E+14	6.8E+07
⁹⁰ Sr	4.2E+00	8.6E+11	1.6E+08
⁶⁰ Co	1.7E-01	5.0E+12	3.0E+06
¹³⁷ Cs	8.8E+00	5.1E+12	3.3E+08
²³⁸ U	3.5E-01	2.4E+12	1.6E+07
²³⁸ Pu	5.6E+00	8.9E+11	2.4E+08
^{239/240} Pu	3.0E+00	8.3E+11	1.1E+08
²⁴¹ Pu	6.4E+01	1.7E+13	2.0E+09
²⁴¹ Am	2.2E+01	7.6E+11	9.7E+08

Table 11: Estimate of maximum activity per nuclide, tank VA002

	Maximum specific activity detected (2013)	WAC maximum total activity per nuclide	Estimate of maximum total activity based on maximum specific activity measured (extrapolated to November 2019)
Radionuclide	Bq/g	Bq	Bq
¹⁴ C	6.0E-01	2.1E+15	2.5E+07
⁶³ Ni	4.5E+00	7.0E+14	1.8E+08
⁶⁰ Co	2.6E+00	5.0E+12	4.3E+07
⁹⁰ Sr	8.7E+01	8.6E+11	3.0E+09
⁹⁹ Tc	2.6E+00	5.4E+13	1.1E+08
¹³⁷ Cs	1.5E+02	5.1E+12	5.3E+09
²³⁸ U	7.5E-01	2.4E+12	3.1E+07
²³⁸ Pu	2.3E+00	8.9E+11	9.0E+07
^{239/240} Pu	1.6E+00	8.3E+11	5.4E+07

²⁴¹ Pu	2.2E+01	1.7E+13	6.5E+08
²⁴¹ Am	1.0E+01	7.6E+11	4.1E+08
²⁴⁴ Cm	8.0E-01	1.4E+12	2.5E+07

Based on the artificial objectives chosen for this exercise, the outcome of the characterization campaign is the decision that the WAC are met. Depending on the statistical indicators of the reporting required for meeting the WAC, the total activity is reported as a quantile estimation, e.g. 95%.

As discussed in this section, the WAC criteria are shown to have been met and therefore the objective of the campaign is reached. No further sampling is therefore needed.

In the context of the INSIDER project, additional samples have been collected, but this has been done independently, without any inputs from the results of the “data analysis of pre-existing data on the sampling design” (i.e. way of sampling, number of samples taken, etc.): the further analysis in this case is performed for the purpose of working through the overall strategy.

2.5 Sampling design

As discussed above, in practice additional sampling is not needed here. However, in the hypothetical case that the objectives are not met and additional information would be required, a sampling design would have to be drawn up at this stage. This is discussed briefly below and outlined in INSIDER deliverable 3.4 ([von Oertzen et al, 2019](#)).

The first step in the sampling campaign should be the establishment of the approximate distribution of the activity in the tanks by external gamma spectrometry or by collimated dose rate measurements. The prerogative here would be to determine if there is an elevation profile in activity concentration within the tanks, for example as a result of solids with more significant radionuclide content settling to the bottom of the tanks, hence this campaign should be performed prior to mixing, and after allowing as long a settling time as possible. This is likely to give an indication of the separation within the tanks between liquid and sludge portions of the waste, and therefore also allow an estimate of the respective quantities of sludge and liquid present.

For tank VA002, the sampling data suggested better homogeneity between the samples. Nevertheless, the same technique should be used to determine whether an elevation profile can be determined exterior to the tank prior to mixing.

Following non-destructive gamma dose rate measurements, there will be an indication of whether the contents are fairly homogeneous with respect to specific activity, or whether there is a significant elevation profile.

In case of an elevation profile, biased sampling should be performed on that portion of the waste with the highest activity contained, prior to performing any mixing. The number of samples to take may be limited by access of the different levels within the tank, but a minimum number of samples of about 6 may be sufficient for confirming the usefulness and applicability of previously identified scaling factors.



In case of no elevation profile, sampling can skip the previous step (biased sampling) and can proceed to unbiased sampling, which should be performed after mixing tank contents. If possible, unbiased sampling should be performed in a way as to ensure that any part of the tank contents is equally likely to be sampled.

Therefore, only the probabilistic sampling method can now be used for sampling the sludge. To ensure a valid random sampling campaign for the entire volume, it has to be ensured

- that the entire mobilisable volume of the tank is circulated during the sampling campaign and
- samples are taken from (nearly) equal volumes from the whole stream.

If biased sampling prior to mixing was skipped, the number of samples of this step will need to be sufficient for determination of scaling factors and range of nuclide factors, otherwise the number of samples still required for the unbiased sampling step can be correspondingly reduced, as the biased sampling data can provide some information about the results to be expected after mixing.

Statistic evaluation of results will be done concerning univariate analysis only with respect to the nuclide specific activity concentration. In addition, the scaling factors of DTM to ^{137}Cs will be evaluated or confirmed.

Based on the pre-existing data, it can be expected (but needs confirmation) that no activity elevation profile can be found for tank VA002, while for tank VA001, an elevation profile is likely but also needs confirmation. If an elevation profile exists, biased sampling will confirm this, and the sampling data can be contributed to the data set used for characterization. If no elevation profile is identified, non-biased sampling only will need to provide sufficient data for characterization.

2.6 Conclusions on data analysis

In this use case, there were no clear objectives for the characterization campaign. We decided to choose as artificial objective the decision if the material will meet the WAC for final disposal, based on disposal conditions in Germany.

The pre-existing data set is small, given there are only 12 samples each for the two tanks to be characterized. Exploratory data analysis indicated that for the purpose of a decision on the stated WAC, the representativity of the data is sufficient. We confirmed this using bootstrap sampling. In tank VA001, bootstrap sampling was much more stable in those cases with outliers after removing those outliers. The tank VA002, there were no outliers present, and bootstrap sampling demonstrated representativeness of the data set.

We performed probabilistic law fitting on data measurements for those radionuclides that exceeded the detection limit for some or all of the samples, to compare the effect of different methods on the estimation the mean values used for deciding if the WAC are met. These comparisons show which method provides the most conservative estimate, which can be important if a decision based on prescribed confidence levels is required.

In both cases, the objective was achieved without further sampling required.

3 Stage 2: Additional INSIDER measurements: data gathering, data analysis and comparison with stage 1 results

Additional data were collected within the context of the INSIDER project. By project design, this data collection was to follow the sampling plan designed in Section 2.5. In practice, this could not really be implemented as data collection and sampling plan development were performed in parallel and therefore independently.

For this use case, the newly collected data is used to make a comparison with the historical data in view of reaching insight on the representativity of the new versus the historical samples. Considering the time elapsed since the first set of data was collected and the settling of the tank contents in the meantime, the expectation would be that the newly collected samples will be less representative of the tank contents because of the presumed development of inhomogeneity within the tanks.

3.1 On-site comparison exercises

Two types of in situ measurement campaign were compared for UC1: dose rate measurements and gamma spectrometry measurements. These are described in detail in deliverable D5.4 ([Herranz et al, 2020](#)). Clear instructions were given to participants on measurement locations, shielding and collimation, calibration, expected outputs and number of replicates. Six collaborators participated in the exercises.

The time elapsed after filling the tanks is approximately seven to eight years. Although the tanks are equipped with stirrers to mix contents, contents have reportedly settled and solidified at the bottom of the tanks.

3.1.1 Dose rate measurements

Dose rate measurements were performed on the two tanks at ISPRA, at pre-determined positions.

Both tanks were measured, and measurements were to be carried out at the back of the tanks, due both to accessibility problems and also to avoid an influence on the measurements of the small ILLW tank situated in the building.

A total number of 7 measurement points was prescribed, five of them located along a vertical line along the middle of the tanks as shown in Figure 22. In the middle location (location "3"), a measurement each is performed a specified distance above and below the horizontal measuring line, which is situated 1 m above ground level and below the fluid line of either tank. Fluid levels for the two tanks differed slightly, with tank VA001 at 1927 mm and tank VA002 at 1670 mm above ground level.

At each location, 5 measurements were performed. This process was repeated 5 times at each location, leading to a total of 25 measurement results per measurement location.

Each measurement was repeated five times. The average values of the measurements, where available, are summarised in Table 12. It shows that the dose rate measurements tended to be comparable, the maximum standard deviation between measurements being about 16%.

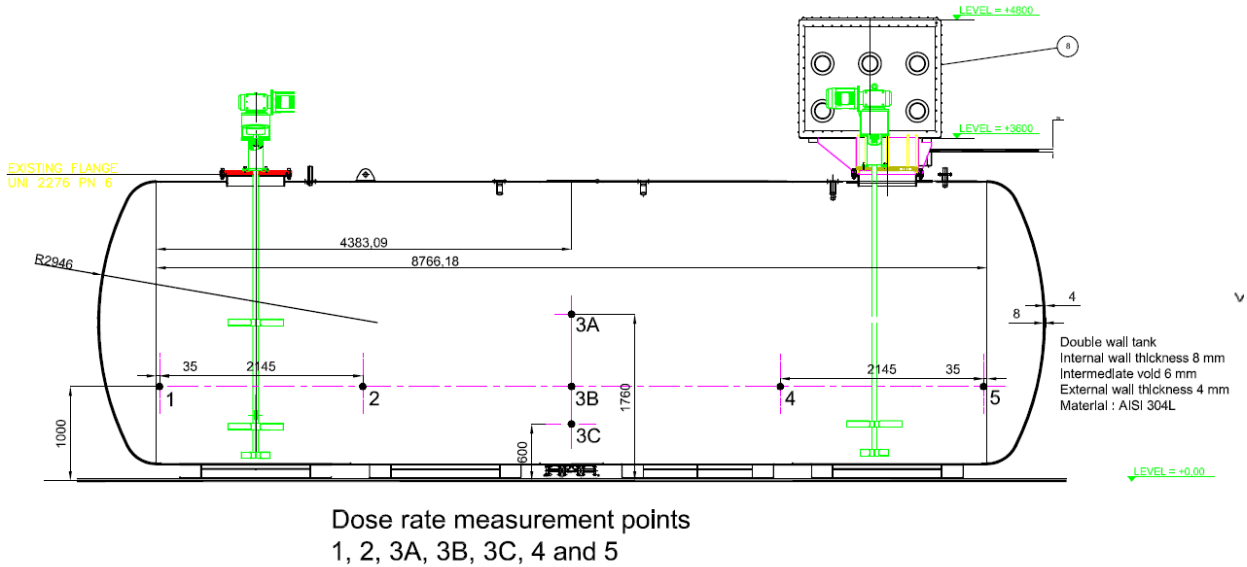


Figure 22: Measurement positions on the tanks for dose rate measurements

Table 12: Summary of dose rate measurements performed in the in situ campaign

Collaborator	Instrument used	tank VA001, average measurement in $\mu\text{Sv/h}$							tank VA002, average measurement in $\mu\text{Sv/h}$						
		1	2	3A	3B	3C	4	5	1	2	3A	3B	3C	4	5
MTA-EK	RadEyeB20	not reported													
UPV/EHU	451P Ion Chamber Survey Meter by FLUKE	0,25	0,28	0,21	2,82	14,94	0,25	0,18	0,57	3,37	3,65	13,39	18,51	12,24	10,64
KIT	FH-40 GL10	0,29	0,30	0,21	4,05	18,9	0,27	0,21	0,50	3,27	2,86	12,8	19,5	13,1	12,7
ONET	AT1123 survey meter	0,30	0,31	0,28	3,00	17,3	0,31	0,24	0,56	3,20	4,10	14,9	20,3	13,7	12,7
Tecnatom	BGO scintillator	0,27	0,28	0,23	2,83	16,7	0,27	0,19	0,53	2,88	3,85	14,6	19,9	13,0	11,7
Mirion	Colibri with VLD/STTC probe	0,29	0,29	0,24	3,52	16,0	0,28	0,24	0,56	3,08	3,53	12,6	17,9	11,7	11,1
Standard deviation, % of mean		7	5	12	16	9	8	13	5	6	13	8	5	6	8

The measurements are compared in Figure 23, confirming the comparability of the instruments and techniques.

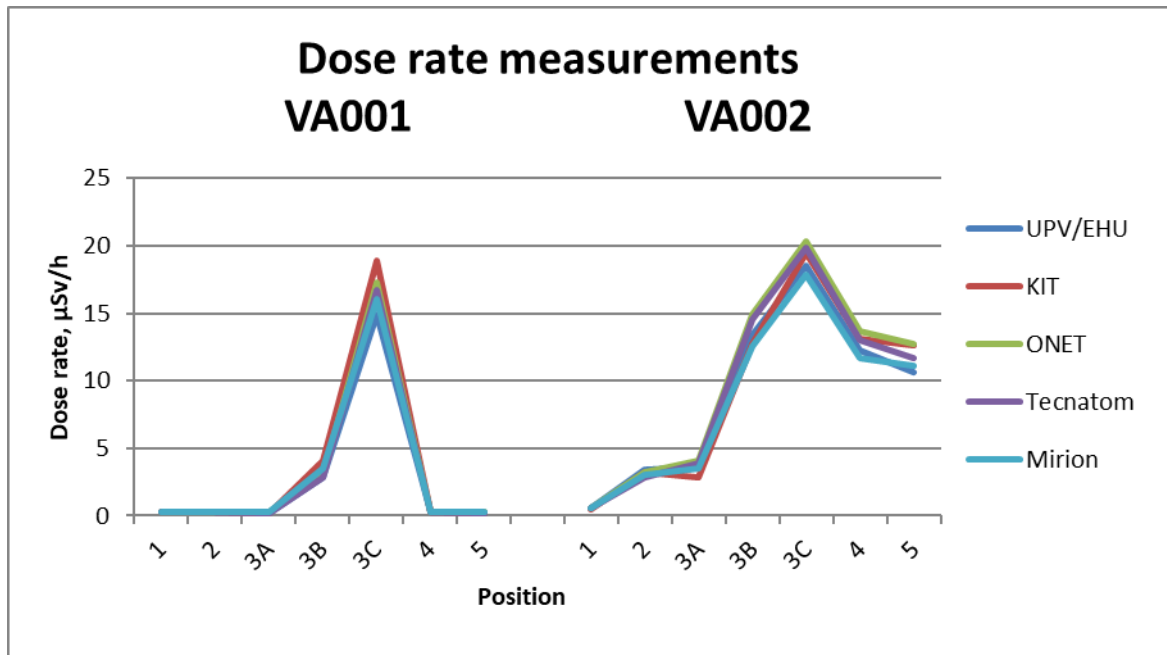


Figure 23: Dose rate measurements, UC1 (left: tank VA001, right: tank VA002)

The results offer good opportunity for the comparability of the different instruments. However, in terms of locating hot spots or inhomogeneities within the tanks, the number of locations was not sufficient.

Inspection of the dose rate profiles in Figure 23 confirms the highest dose rate at position 3C for both tanks. As this position is situated close to the bottom of the tank, this is an indication of an elevation profile of activity distribution, with the highest specific activity being present at the bottom of the tank. This can be confirmed by inspection of the horizontal and vertical dose rate profiles in the two tanks, shown in Figure 24. As suspected, the dose rate increases towards the bottom of the tanks, confirming a consolidation of the activity at the bottom of both tanks. However, the vertical profile also shows an interesting trend: in tank VA001, the dose rate at the center of the tank is elevated, while in tank VA002 there is also an increase in the dose rate from left to right, moving from position 1 towards position 5, again with the maximum of the dose rate at the center.

The maximum dose rate at the center of the tank could be explained by scattering, as the amount of material contributing to the dose rate is highest in the center of the tank. However, the horizontal profile seen in tank VA002 with an increase towards one end of the tank must have a different explanation; here there seems to be some consolidation of the activity towards one end of the tank, perhaps by stirring contents only at one end of the tank.

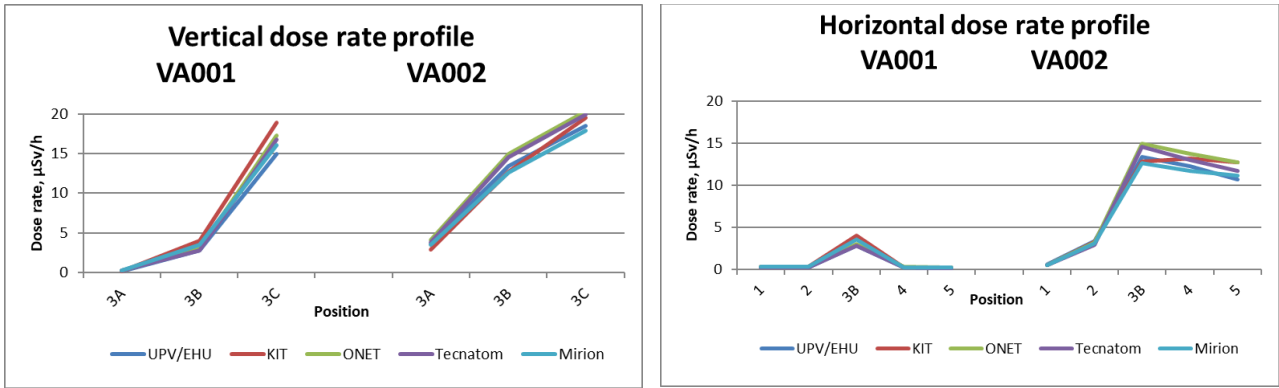


Figure 24: Vertical (left) and horizontal (right) dose rate profiles in both tanks

3.1.2 Gamma spectrometry measurements

On each of the two tanks, gamma spectrometry measurements were performed at two vertically displaced positions respectively, as shown in Figure 25. The elevation of the bottom collimator is slightly lower in tank VA001 compared to tank VA002.

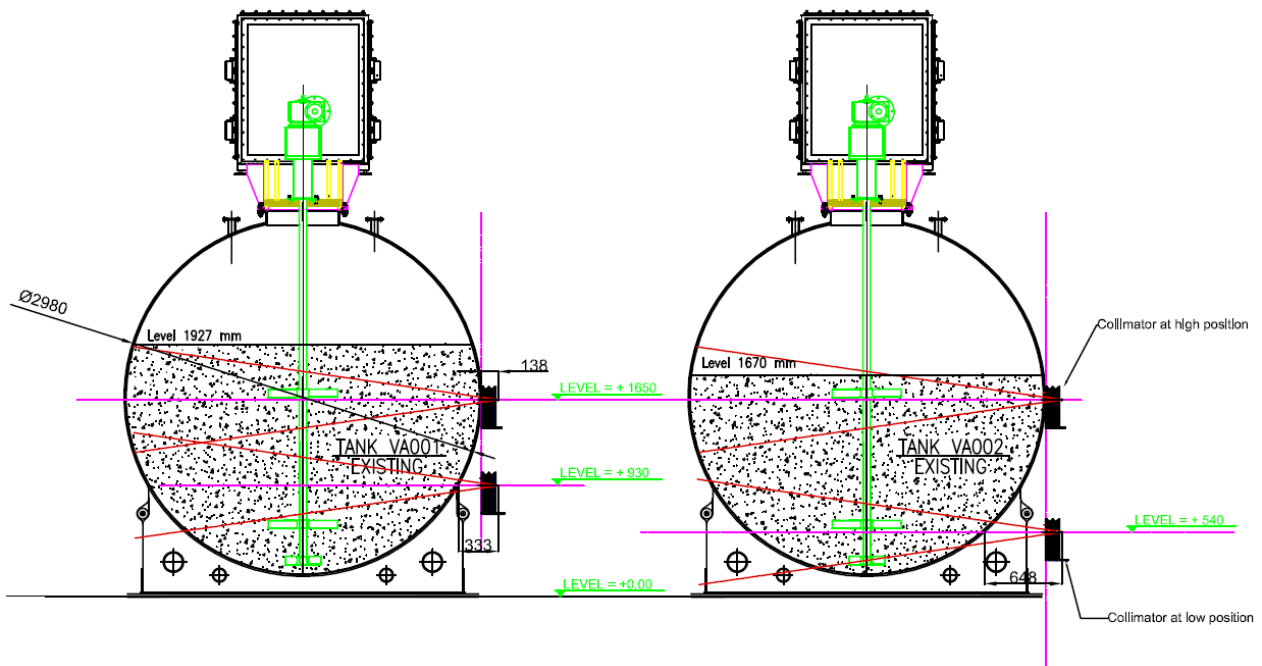


Figure 25: Measurement positions for gamma spectrometry measurements (left: tank VA001, right: tank VA002)

The results were used to report the activity of the dominant nuclides ^{137}Cs and ^{60}Co in the tanks and then determine their ratio. The results are summarised in Table 13.

Table 13: Summary of gamma spectrometry measurements (November 2019)

		ratio $^{137}\text{Cs}/^{60}\text{Co}$			
		tank VA001		tank VA002	
Collaborator	Instrument used	top	bottom	top	bottom
MTA-EK	Canberra GL2020 HPGe	not reported			
UPV/EHU	LaBr3 scintillation counter by Mirion CZT semiconductor gamma-ray spectrometer	121,2	156,8	140,3	144,1
KIT	CdTe detector				
ONET	Ge detector	161,6	142,9	129	185,8
	CZT detector	159,3	145,0	127,9	183,3
Tecnatom	CZT detector	131	116	120	132
Mirion	LaBr detector	157	175	156	-
standard deviation, % of mean		14	17	11	18

While the difference between the measurements of the activity ratio $^{137}\text{Cs}/^{60}\text{Co}$ displays a moderate standard deviation of at most 18 %, the difference in the individual results of these measurements is significant, as the final result is based not only on the interpretation of the spectrometry peak but also on the modelling of the total activity based on the geometry of the tanks. The difference using a specific method but based on a different geometry is a factor of up to 4 between positions on the same tank. However, no clear conclusion is possible on the trend between the top and the bottom of the tanks, as shown in Figure 26. The different labs display different outcomes, with some reporting an increase from top to bottom, and some a decrease, for tank VA001. For tank VA002, each of the labs reports an increase from top to bottom in the ratio reported, even though the ratios vary considerably. The trend is also not uniform between the two tanks: for example, ONET reports a decrease from top to bottom in tank VA001 and an increase in tank VA002, while Tecnatom reports the opposite effect.

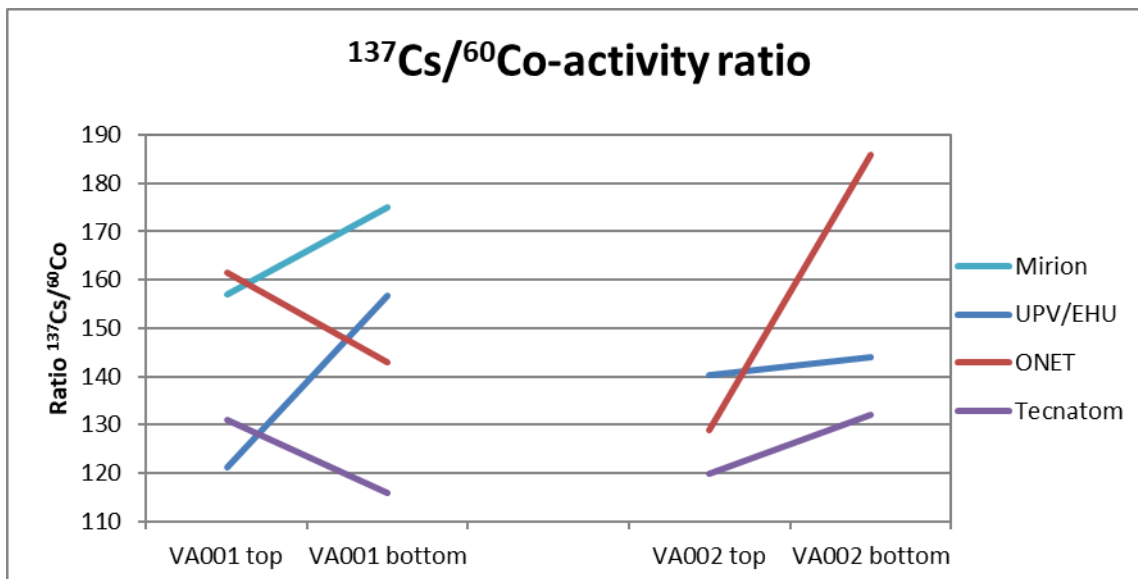


Figure 26: Activity ratio $^{137}\text{Cs}/^{60}\text{Co}$ in the two tanks, as determined by gamma spectrometry

The gamma spectrometry measurement campaign confirms the finding from the dose rate exercise: the distribution of activity within both tanks is not homogeneous, with a concentration of activity at the bottom through settling of the solid portion of the contents. This factor leads to significant differences in estimations for the activity ratio between ^{137}Cs and ^{60}Co , depending on the position of the measurement. However, because the activity ratio between ^{137}Cs and ^{60}Co is calculated at a fixed position for both nuclides in the ratio, the difference between results at different positions is less enhanced than those for the dose rate, which is an absolute measurement value instead.

3.2 Sampling and in-lab intercomparison exercise

The results of the interlaboratory comparison exercises are reported in deliverable D6.3, part 4. Several laboratories participating in the interlaboratory comparison (ILC1') exercise on the real samples from ISPRA's tank VA002 observed that there were big issues of homogeneity between the 2 samples received from ISPRA. The uncertainty related to the homogeneity is of the order of several tens of percent. This is a major problem for the interlaboratory comparison as the analysis of the measurement results will be meaningless.

For this reason, in agreement with the project leader in charge of the production of reference materials for the INSIDER project, this particular interlaboratory comparison was cancelled.

3.2.1 Benchmarking exercise on real samples

To make up for the cancellation of the interlaboratory comparison on samples from the tanks, an alternative comparison was organised on a certified reference material (CRM) which is a liquid material, CRM1, based on UC1 (liquid effluent tank waste from JRC Ispra) and produced by WP4. With regard to uncertainties, the main results of this comparison are summarised in Table 14.

analytical method characteristics						
			trueness	precision		
measurand	analytical method	level (Bq/g)	En	repeat. sr	repro. sR	U measurement uncertainty (k=1)
Am-241	γ spec.	9.3	-0.1	1.5%	2.7%	3.2%
Co-60		9.1	-1.0	2.0%	4.8%	5.1%
Cs-137		18	-0.6	2.5%	4.7%	5.2%
Am-241	α spec.	9.3	-1.0	4.6%	4.7%	5.1%
Pu-238		2.3	-0.3	4.6%	5.7%	6.4%
Pu-239		1.3	1.4	5.7%	8.7%	11%
U-238		1.4	0.2	4.3%	9.5%	12%
Fe-55	LSC	3.3	1.4	8.2%	19%	21%
Ni-63		3.6	-0.05	5.5%	20%	23%

Table 14: Measurement uncertainty from comparison on CRM1

As expected for measurements in laboratory, the measurement uncertainty of γ spectrometry is the lowest in the order of 5% (k=1) for an activity level of 10 - 20 Bq/g (Am-241, Co-60, Cs-137). The measurement uncertainty by α spectrometry is in the order of 5 to 12% (k=1) for levels of 10 and 1 Bq/g respectively (Am-241, Pu-238, Pu-239, U-238). For liquid scintillation measurements (LSC), which are probably the most difficult methods to implement in laboratory, the measurement uncertainty is of the order of 20% (k=1) for a level of about 3 Bq/g (Fe-55, Ni-63).

4 Stage 3: Comparison additional INSIDER measurements with data analysis on pre-existing data

4.1 Comparison between activity ratios based on in-situ with existing data

The existing data from the original sampling campaign date from 2012 and 2013 respectively. In order to compare these with the gamma spectrometry results from the interlaboratory comparisons, the activity ratios have to be extrapolated for the time elapsed (7 years) since taking the early measurements. In Figure 27, we compare the measured $^{137}\text{Cs}/^{60}\text{Co}$ activity ratio with the ratio calculated by taking the median value of the existing lab samples and extrapolating to the date of the gamma spectrometry sampling (2019). No information is available about the position at which the samples were extracted in the early campaign, but the assumption could be made that immediately following deposition into the tank and mixing, the content would have been fairly homogeneous. The figures show overall consistency between the existing data and the gamma spectrometry measurements. In tank VA001, the lab results report a ratio slightly lower activity ratio than all of the gamma spectrometry measurements, but still within the same order of magnitude. The agreement in the case of tank VA002 is better than that for tank VA001.

While the difference of up to a factor of 2 between existing data and the gamma spectrometry results is quite large, the selected objective is achieved regardless, as the WAC refer only to maximum activities for the various nuclides which are several orders of magnitude below the WAC limits.

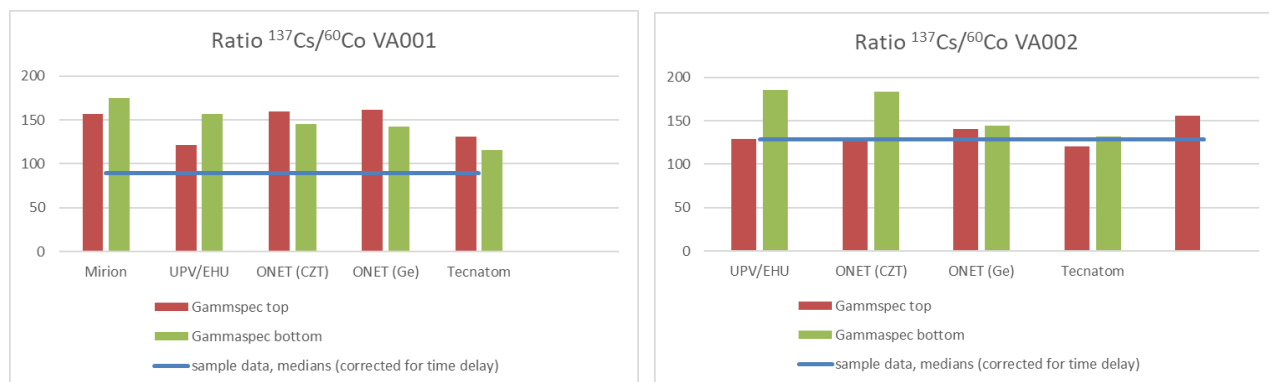


Figure 27: Comparison of activity ratio $^{137}\text{Cs}/^{60}\text{Co}$ between gamma spectrometry measurements and existing data (extrapolated to November 2019)

4.2 Uncertainty evaluation & sensitivity study

In Section 2.3, we analysed the impact of several statistical methods on the estimate of the mean value for the activity of the nuclides measured. The methods included empirical mean, Wilks median, bootstrap estimation of mean, Bayesian estimation and mean estimated from fitted theoretical distribution law. The results were compared between the application of the methods with and without the uncertainty, represented by the limit of detection for the radiochemical analyses. For these, the Wilks method proved to provide the most conservative estimates, particularly so for data sets with outliers.

The representativeness of the data set was checked using bootstrap sampling of 5 to 10 samples from the existing data set. This showed a stabilisation of the data sets at about 10 data points, except in the cases of outliers being present. This demonstrates the importance of verifying outliers to confirm if they are process driven or merely errors.

5 Lessons learnt and impact on the approach

For use case 1, the initial request for characterization did not include clear well-defined objectives. A questionnaire was used initially to gain more information, but this proved insufficient for the purpose. Therefore, we made some assumptions about the intended end points and defined artificial objectives. We assumed that the waste will be conditioned by evaporation and packaged to satisfy the waste acceptance criteria (WAC) for disposal in the Konrad disposal facility for low and medium level radioactive waste in Germany. This provided clear objectives for analysing the data.

The type of objective chosen was the determination of the total activity content of each of the two tanks, so that these can be checked against the total activity limits specified for each nuclide in the WAC. The WAC were then artificially selected as the highest priority objective in the overall strategy.

The initial data set was small: 12 samples each for the two tanks, thus robust methods for exploratory data analysis were used.



Preprocessing of the data and exploratory data analysis provided first trends: for tanks VA001, some outliers were identified, while data for VA002 did not present clear outliers. In the univariate data set, no spatial trends were identified in the initial data set. However, after the significant time lapse since then, an elevation profile in the tanks was suspected and confirmed during the in situ dose rate measurements performed. Sampling for the initial data, which was performed immediately following the filling of the tanks, was probabilistic. The additional data collected in the context of the INSIDER project in November were no longer probabilistic but rather convenience sampling, as there was no process available to sample tanks contents at pre-determined elevations (i.e. constraint on possible sampling locations).

The ETM radionuclides detected above the detection limits are, for both tanks, the gamma emitters ^{90}Co , ^{137}Cs and ^{241}Am . In the case of tank VA001, the DTM nuclide ^{90}Sr could be estimated via correlation to ^{60}Co , ^{238}U via ^{137}Cs and the nuclides ^{241}Pu , ^{238}Pu and $^{239+240}\text{Pu}$ via correlation to ^{241}Am . Therefore, in this case the estimation of the total activity content would be possible via measurement of the ETM nuclides only by extrapolation using the correlation factors. This is graphically confirmed in the PCA analysis performed (Figure 8), which clearly shows two correlation clusters, one containing ^{90}Sr , ^{60}Co , ^{238}U and ^{137}Cs and another containing ^{238}Pu , ^{241}Pu and $^{239+240}\text{Pu}$. Representativeness of the ETM nuclides could be confirmed with a bootstrap analysis of the small data set reaching stability at a data size of about 10. The same analysis for the DTM nuclides was not as successful for the DTM nuclides ^{241}Pu , ^{238}Pu , ^{238}Pu and $^{239+240}\text{Pu}$ on account of the presence of outliers in the data sets. Removing the outliers from the data set for the bootstrap analysis removed this complication. The estimation of the mean activity and 90% quantile for the activity could be performed with the small data set at hand. For meeting the WAC defined, the existing data are therefore likely sufficient, with additional measurements possibly restricted to the conditioned waste package, for the determination of dose and surface dose rate data.

In the case of tank VA002, the estimation of the total activity via correlation factors was not possible, as the only DTM nuclides for whom correlations with ETM nuclides could be found were $^{238+240}\text{Pu}$ (with ^{60}Co) and ^{238}U (with ^{137}Cs). Graphical confirmation of this lack of correlation is demonstrated in the PCA analysis (Figure 14). The representativeness of the data could be confirmed via bootstrap analysis which reached stability at a data size of about 10. The estimation of the total activities could be completed using the probabilistic risk bound method calculating the probability of exceeding predefined limits. In this case, because of the lack of correlation between ETM and DTM nuclides, additional data are likely required but depend on the specific limits set by the WAC. The results provided by the study of this use case show that, in particular for tank VA001, taking into account measurement of uncertainties and information on limits of detection can have a considerable impact on activity estimations even with small data sets. These outcomes have to be taken into consideration for D&D scenarios, in particular for the categorization and forecasting of waste volumes. Nevertheless, for risk analyses by estimation to exceed a given threshold, with small data sets, it is more robust to use probabilistic risk bound method.

Pre-processing and exploratory analysis of the existing data already confirmed that the WAC could be met. Secondary objectives included meeting the WAC for secondary parameters such as external dose rate and chemical composition. At this stage, all objectives were met and the development of sampling strategy and gathering of additional data would not have been required. Within the context



of the INSIDER project, the sampling strategy developed was in practice not connected to the sampling performed for the on-site non-destructive analysis and the interlaboratory comparison exercise.

6 Acronyms and abbreviations

ADR:	Accord européen relatif au transport international des marchandises Dangereuses par Route, European Transport Regulations
ALARA:	As low as reasonably achievable
APG:	Abfallproduktgruppe = waste product group
DA:	Destructive analysis
D&D:	Decommissioning and dismantling
DQO:	Data quality objectives
DTM:	Difficult to measure
EUG:	End user group
ETM:	Easy-to-measure
IAEA:	International Atomic Energy Agency
JRC:	Joint Research Center
LOD:	Limit of detection
LLD:	Lower than limit of detection
LLLW:	Liquid Low Level Waste
NDA:	Non-destructive analysis
NPP:	Nuclear power plant
NV:	Nuclide vector
QA:	Quality assurance
SF:	Scaling factor
WAC:	Waste acceptance criteria

7 Bibliography

Blatman, G., Delage, T., looss, B., Pérot, N. (2017). Probabilistic risk bounds for the characterization of radiological contamination, EPJ Nuclear Sci. Technol. 3, 23 (2017).

European Commission (2016). Nuclear Decommissioning and Waste Management Programme at the Joint Research Centre, Ispra Site, Joint Research Centre.

Herranz, M., et al (2020). INSIDER WP 5 – In situ measurements: Reporting on in situ measurement campaigns Deliverable D5.4.

- International Atomic Energy Agency (1998). Radiological Characterization of Shut Down Nuclear Reactors for Decommissioning Purposes, IAEA Technical reports series No. 389, IAEA, Vienna.
- International Atomic Energy Agency (2009). Determination and use of scaling factors for waste characterization in nuclear power plants, IAEA Nuclear Energy Series No. NW-T-1.18, IAEA, Vienna.
- Londyn, P. (ENVINET) (2013a). Final Chemical and Radiological Analysis Report, Work Package 03-2011, 2013.
- Londyn, P. (ENVINET) (2013b). Final Chemical and Radiological Analysis Report, Work Package 04-2012, 2013.
- NEA (2013). Radiological Characterisation for Decommissioning of Nuclear Installations, Final Report of the Task Group on Radiological Characterisation and Decommissioning (RCD) of the Working Party on Decommissioning and Dismantling (WPDD), NEA/RWM/WPDD(2013)2, 2013.
- Peerani P., Boden S., Crozet M., Zanovello F., Herranz M. (2017). Design of the benchmarking exercise, INSIDER WP2 – Requirement and validation, Deliverable D2.5.
- Pérot, N., Desnoyers, Y., Augé G., Aspe F., Boden S., Rogiers B., Sevbo O., Nitsche O., (2017). INSIDER WP3 – Sampling strategy report on the state of the art, Deliverable 3.1.
- Rogiers, B., Boden S., Pérot N., Desnoyers Y., Sevbo O., Nitsche O. (2018). Report on statistical approach, INSIDER WP3 – Sampling strategy, Deliverable D3.2.
- U.S. Nuclear Regulatory Commission (2000). Multi-Agency Radiation Survey and Site Investigation Manual (MARSSIM), NUREG-1575, Rev. 1.
- Brenneke, P. (ed), Bundesamt für Strahlenschutz, Fachbereich Sicherheit nuklearer Entsorgung (2015). Anforderungen an endzulagernde radioaktive Abfälle (Endlagerungsbedingungen, Stand: Dezember 2014)
- Von Oertzen, G. Nitsche, O., Hashymov, A. (2019). INSIDER WP3 – Sampling plans for use case 1, Deliverable 3.4.